NASA/TM–2013-218046

A Storm Surge and Inundation Model of the Back River Watershed at NASA Langley Research Center

Jon Derek Loftis and Harry V. Wang
Virginia Institute of Marine Science
The College of William and Mary
Gloucester Point, Virginia

Russell J. DeYoung
Langley Research Center
Hampton, Virginia

October 2013

NASA STI Program . . . in Profile

Since its founding, NASA has been dedicated to the advancement of aeronautics and space science. The NASA scientific and technical information (STI) program plays a key part in helping NASA maintain this important role.

The NASA STI program operates under the auspices of the Agency Chief Information Officer. It collects, organizes, provides for archiving, and disseminates NASA's STI. The NASA STI program provides access to the NASA Aeronautics and Space Database and its public interface, the NASA Technical Report Server, thus providing one of the largest collections of aeronautical and space science STI in the world. Results are published in both non-NASA channels and by NASA in the NASA STI Report Series, which includes the following report types:

- TECHNICAL PUBLICATION. Reports of completed research or a major significant phase of research that present the results of NASA Programs and include extensive data or theoretical analysis. Includes compilations of significant scientific and technical data and information deemed to be of continuing reference value. NASA counterpart of peer-reviewed formal professional papers, but having less stringent limitations on manuscript length and extent of graphic presentations.

- TECHNICAL MEMORANDUM. Scientific and technical findings that are preliminary or of specialized interest, e.g., quick release reports, working papers, and bibliographies that contain minimal annotation. Does not contain extensive analysis.

- CONTRACTOR REPORT. Scientific and technical findings by NASA-sponsored contractors and grantees.

- CONFERENCE PUBLICATION. Collected papers from scientific and technical conferences, symposia, seminars, or other meetings sponsored or co-sponsored by NASA.

- SPECIAL PUBLICATION. Scientific, technical, or historical information from NASA programs, projects, and missions, often concerned with subjects having substantial public interest.

- TECHNICAL TRANSLATION. English-language translations of foreign scientific and technical material pertinent to NASA's mission.

Specialized services also include organizing and publishing research results, distributing specialized research announcements and feeds, providing information desk and personal search support, and enabling data exchange services.

For more information about the NASA STI program, see the following:

- Access the NASA STI program home page at *http://www.sti.nasa.gov*

- E-mail your question to help@sti.nasa.gov

- Fax your question to the NASA STI Information Desk at 443-757-5803

- Phone the NASA STI Information Desk at 443-757-5802

- Write to:
  STI Information Desk
  NASA Center for AeroSpace Information
  7115 Standard Drive
  Hanover, MD 21076-1320

NASA/TM–2013-218046

A Storm Surge and Inundation Model of the Back River Watershed at NASA Langley Research Center

Jon Derek Loftis and Harry V. Wang
Virginia Institute of Marine Science
The College of William and Mary
Gloucester Point, Virginia

Russell J. DeYoung
Langley Research Center
Hampton, Virginia

National Aeronautics and
Space Administration

Langley Research Center
Hampton, Virginia 23681-2199

October 2013

Available from:

NASA Center for AeroSpace Information
7115 Standard Drive
Hanover, MD 21076-1320
443-757-5802

Table of Contents Page #

LIST OF TABLES Page #

LIST OF FIGURES Page #

ABSTRACT

Sub-grid modeling is a novel method by which inundation on the sub-grid level can be obtained through the combination of water levels and velocities efficiently calculated at the coarse computational grid, the discretized bathymetric depths, and local friction parameters without resorting to solve the full set of equations. The Sub-grid approach essentially allows velocity to be determined rationally and efficiently at the sub-grid level. This salient feature enables coastal flooding to be addressed in a single cross-scale model from the ocean to the upstream river channel without overly refining the grid resolution. The sub-grid model is suitable for hydrologic transport model coupled with high-resolution lidar topography for the NASA Langley Research Center for use in modeling storm surge inundation including precipitation-induced flooding.

To this end, high-resolution digital elevation models (DEMs), incorporating GIS from Lidar-derived topography, were used for incorporation into a sub-grid model, for research into case studies related to recent substantial inundation events at the NASA Langley Research Center in Hampton, VA. Two inundation events were modeled. The 2003 Hurricane Isabel was utilized for a comparison of inundation extent including and without precipitation included in the sub-grid model, in addition to sea level rise projections associated with global climate change for Isabel+00in (Hurricane Isabel's maximum extent of inundation), Isabel+15in, Isabel+30in, Isabel+60in. Also the 2011 Hurricane Irene confirmed that sub-grid model results accurately predicted the maximum extent of inundation at Langley Research Center via spatial comparison of NASA-recorded GPS wrack line data at 6 different sites. The model provided accurate water level prediction with maximum extent of the inundation within a few tens of meters to the wrack line measurement. Further improvement was made when the infiltration by the pervious and impervious surface were taken into consideration.

1. Introduction

Located in Hampton, Virginia, Langley Research Center is adjacent to the banks of the Chesapeake Bay, making it susceptible to hurricanes and extreme coastal weather brought up from the Gulf Stream. Langley covers over 800 acres (20 acres located on the Langley Air Force Base) and is surrounded by the Back River, a shallow estuarine inlet of the Chesapeake Bay, the largest estuary in the United States.

Langley Research Center is located in one of the most vulnerable areas in the United States to the effects of climate change and sea level rise. The East Coast has 50% of its length in the "very high" or "high" vulnerability range. The highest vulnerability areas are typically coastlines where the regional coastal slope is low and the major landform type is a barrier island. A significant exception to this is found in the lower Chesapeake Bay. Here, the low coastal slope, vulnerable landform type (salt marsh), and high rate of relative sea-level rise combine for a high coastal vulnerability. This threat requires the use of high-resolution inundation modeling to assess the flooding damage to Langley infrastructure on a building-by-building basis for a suite of potential storms from nor'easters to hurricanes. This is especially relevant to the construction of "New Town"; the new building plan for this century.

The Chesapeake Inundation Prediction System (CIPS) has been developed and demonstrated to provide a capability to forecast large-scale storm surge and land area inundated in the Chesapeake Bay (CIPS final report, 2011, Cho et al. 2011; Roland et al. 2012). Recently, sub-grid modeling capability was added to the model framework in order to incorporate fine-scale features (within 1-5 meters) into the coarse base grid without significantly increasing overhead to computing resources (Casulli and Stelling, 2011). Sub-grid modeling is a cutting-edge approach which is designed to incorporate Lidar topography into the sub-grid of an otherwise regular model framework to simulate storm surge and inundation (Figure 1.1).

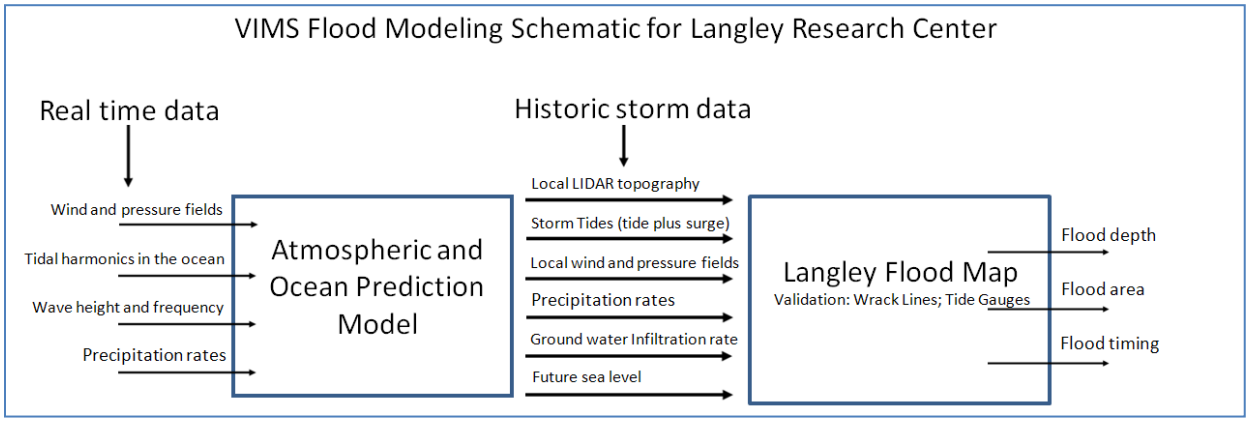

Figure 1.1. VIMS flood modeling methodology for NASA Langley Research Center. The focus of this paper is the Flood Map Modeling using Lidar-derived topography to produce the high-resolution Langley flood map. In future modeling an Atmospheric and Ocean Prediction Model would be added to give near real time flood maps.

The topographic representation (stored in the model sub-grid) will allow the effects of friction and total conveyance to be determined more accurately, resulting in better characterization of total inundation.

This new methodology is significant because it provides a rational way to combine high-resolution Lidar and bathymetry data into the model, and concurrently generate storm surge and hydrological transport model results. At Langley a network of numerous ditches, on the order of 2-5 meters wide, are utilized for draining excess water during weather events as shown in Figure 1.2. These ditches are part of the hydrological features that need to be resolved in the model in order to predict the extent, depth, and the timing of the flood inundation (Figure 1.1). Utilizing the sub-grid approach, it is possible to resolve the ditches that are on the order of a few meters wide as shown in Figure 1.3A-B, and at the same time be able to channel the rainfall into runoff to simulate the water budget and inundation for the entire Back River system influenced via external forcing.

This paper will describe an advanced sub-grid inundation model of NASA Langley which will incorporate the flowing topics:

A. Retrieve the high-resolution Lidar data and incorporate it into the sub-grid model

B. Set up the sub-grid model and incorporate precipitation during major storm events

C. Perform calibrations and conduct hindcast for recent major inundation events

D. Incorporate sea level rise scenarios

This work demonstrates that sub-grid modeling technology (now as part of Chesapeake Bay Inundation Prediction System, CIPS) can incorporate high-resolution Lidar measurements provided by NASA Langley Research Center into the sub-grid model framework to resolve detailed topographic features for use as a hydrological transport model for run-off simulations within NASA Langley and Langley Air Force Base. The rainfall over land accumulates in the ditches/channels resolved via the model sub-grid was tested to simulate the run-off induced by heavy precipitation. Possessing both the capabilities for storm surge and run-off simulations, the CIPS model was then applied to simulate real storm events starting with Hurricane Isabel in 2003. It will be shown that the model can generate highly accurate on-land inundation maps as demonstrated by excellent comparison of the Langley tidal gauge time series data (CAPABLE.larc.nasa.gov) and spatial patterns of real storm wrack line measurements with the model results simulated during Hurricanes Isabel (2003), and Irene (2011). With confidence built upon the model's performance, sea level rise scenarios from the ICCP (International Climate Change Partnership) were also included in the model scenario runs to simulate future inundation cases.

The model methodology and setup are discussed in Appendix A. Here the development of a hydrological transport simulation with included precipitation is developed in detail.

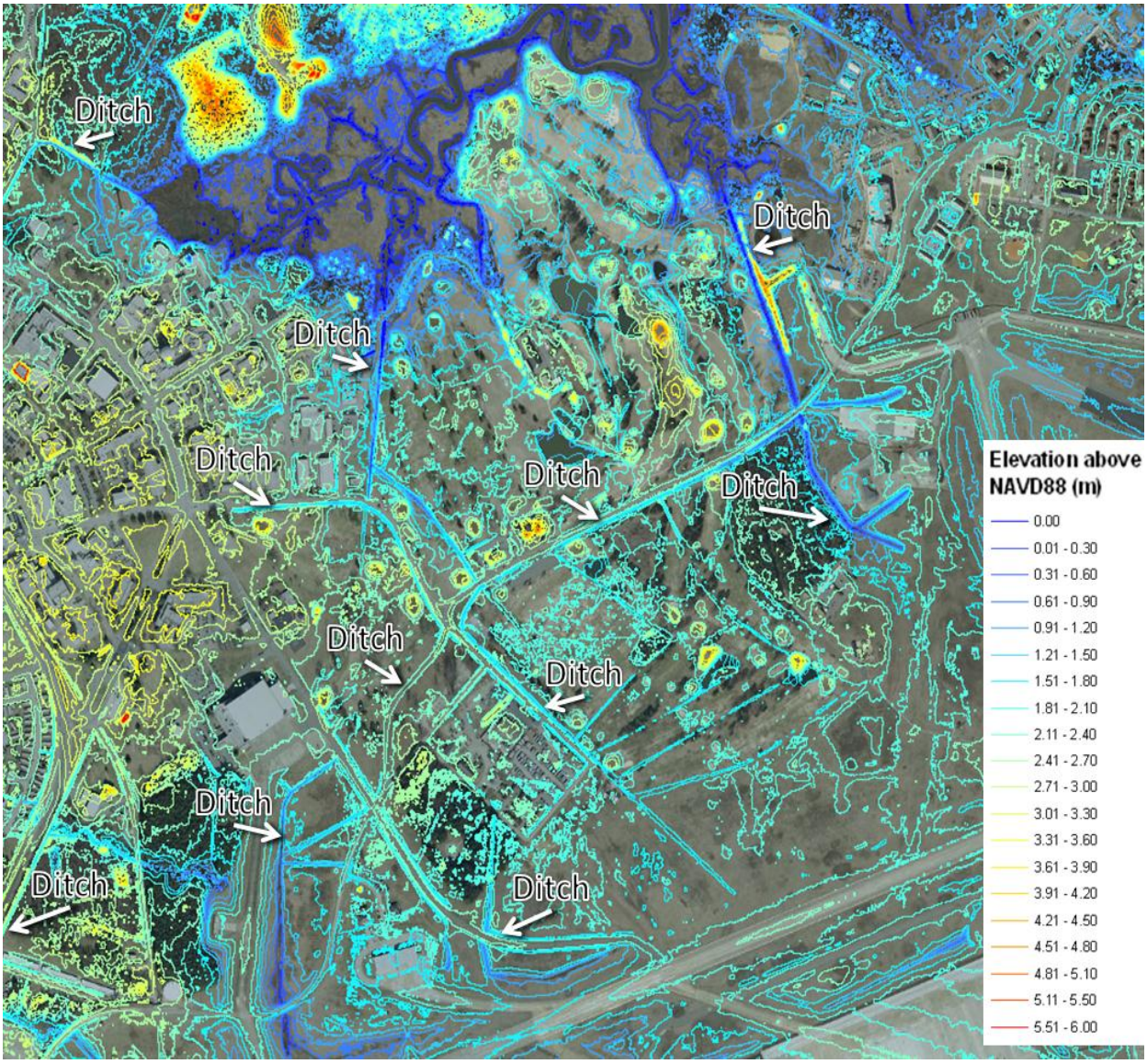

Figure 1.2. Lidar contour data for Langley Air Force Base (right) and NASA Langley Research Center (Left) on the Back River peninsula. North is upward. Ditches are labeled which inpact innundation modeling. Elevation above NAVD88 is shown in color and indicates the near sea level height of the Center.

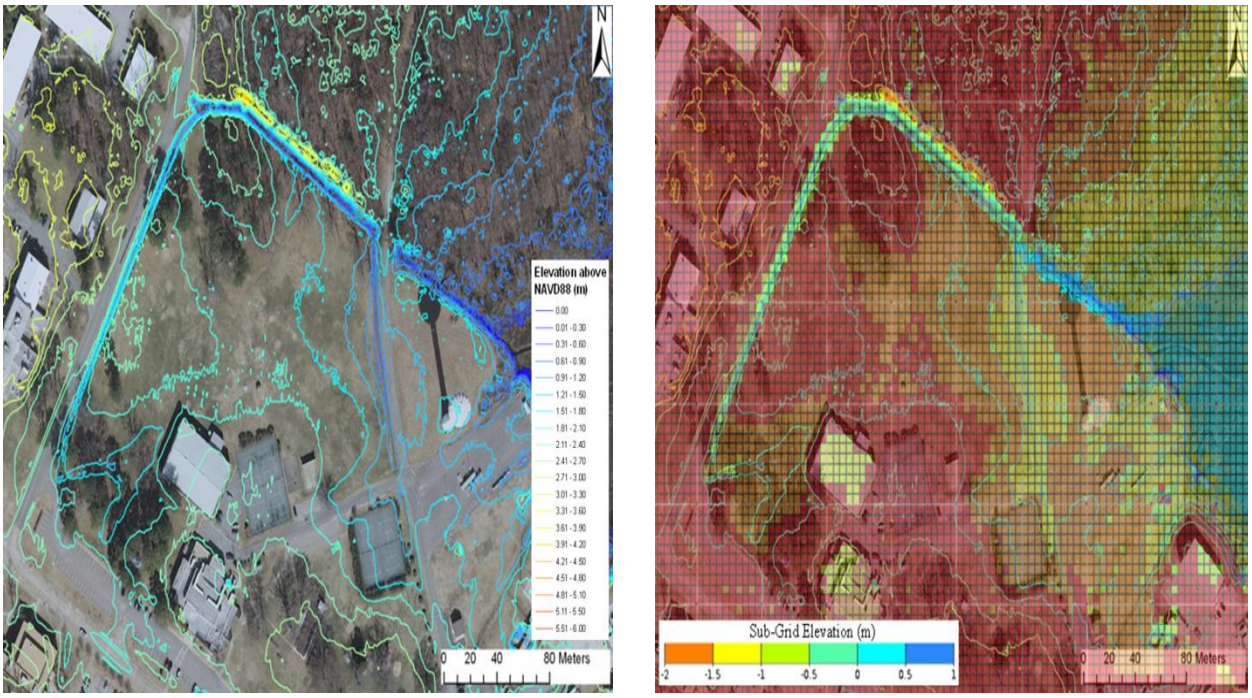

Figure 1.3A. Lidar resolved ditch contours (0-6 ft) adjacent to Doolittle Rd. near Building 1222 draining into west end of Tabb Creek (left); 50m Base Grid (grey lines) with 5m nested Sub-grid (black lines) displaying elevation with superposed Lidar contours (right). (Scale as Fig. 1.2)

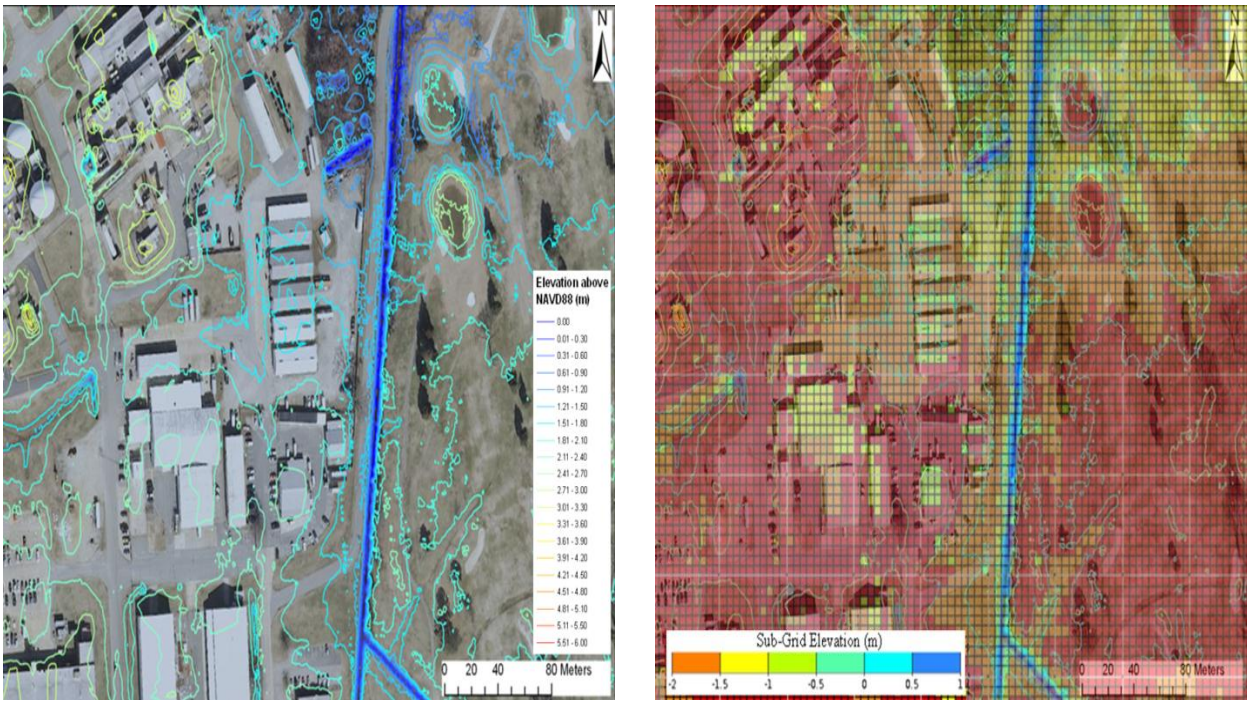

Figure 1.3B. Lidar resolved ditch contours (0-6 ft) adjacent to Gregg Rd. leading to Eaglewood Golf Course draining into south end of Tabb Creek (left); 50m base grid (grey) with 5m nested Sub-grid (black lines) superposed with Lidar elevation contours (right).

2. Model Hindcast for the Back River Estuary

2.1 Results for 2003 Hurricane Isabel

A peak precipitation rate of 28 mm/hr was observed during Hurricane Isabel on September 18, 2003, at 20:00 GMT as shown in Figure 2.1. A time series comparison of observed results at Sewell's Point and sub-grid results yielded an observed peak of 2m above mean sea level as shown in Figure 2.2. Correlation of observation data against the model prediction yielded an $R^2 = 0.9903$ for 2003 Hurricane Isabel and gave confidence that the model was working properly.

2.1.1 Inundation Model Comparison with and without Rainfall

Rainfall is an important parameter to consider in inundation modeling. A considerable gap currently exists between atmospheric modeling and hydrodynamic modeling communities. To appropriately address tropical and extra-tropical storm systems for both flooding extent and duration, precipitation is an invaluable parameter for modeling in the coastal plane. In an area like NASA Langley Research Center and Langley Air Force Base, where the terrain is converted lowlands and salt marshes, virtually no buffer exists between an impending storm surge intruding into the Back River estuary.

Precipitation is useful to consider in flood modeling for considering relatively flat terrain like the terrain at NASA Langley where the water table is regularly high (close to the exposed soil surface) throughout the year. Considering inundation thickness (height of water above the topographic land surface) is a useful method for evaluating the importance of coding precipitation into a hydrodynamic model as a model input. Figure 2.3A displays the maximum inundation thickness around NASA Langley Research Center and Langley Air Force Base after the 2003 Hurricane Isabel in a simulation neglecting precipitation. In contrast, Figure 2.3B illustrates the maximum inundation thickness in meters for 2003 Hurricane Isabel including precipitation input over the Back River peninsula.

Upon inclusion of precipitation data as an atmospheric model input, the model identified localized flooding non-contiguous to the storm surge flooding associated with 2003 Hurricane Isabel. Specific areas of localized precipitation-based flooding persist in the southwest region of NASA Langley and the central to southwest regions of Langley Air Force Base. There are interior areas along the western edge of the Langley Research Center (which are not directly adjacent to the storm surge-induced flooding along the edge of the Back River estuary) that are now shown to be inundated when precipitation is included. While some of these areas non-contiguous with the Back River estuary are local drainage infrastructure containing a water thickness of 25cm or less, many areas in the southwestern portion of the map near Langley Air Force Base (approaching the NASA Hangar) are inundated by precipitation-derived flooding between 1.00-1.75m. This is effectively exemplified in the difference map shown in Figure 2.3C. Note that Figure 2.3C is the difference of Figure 2.3B minus Figure 2.3A, generated by ArcGIS10.1.

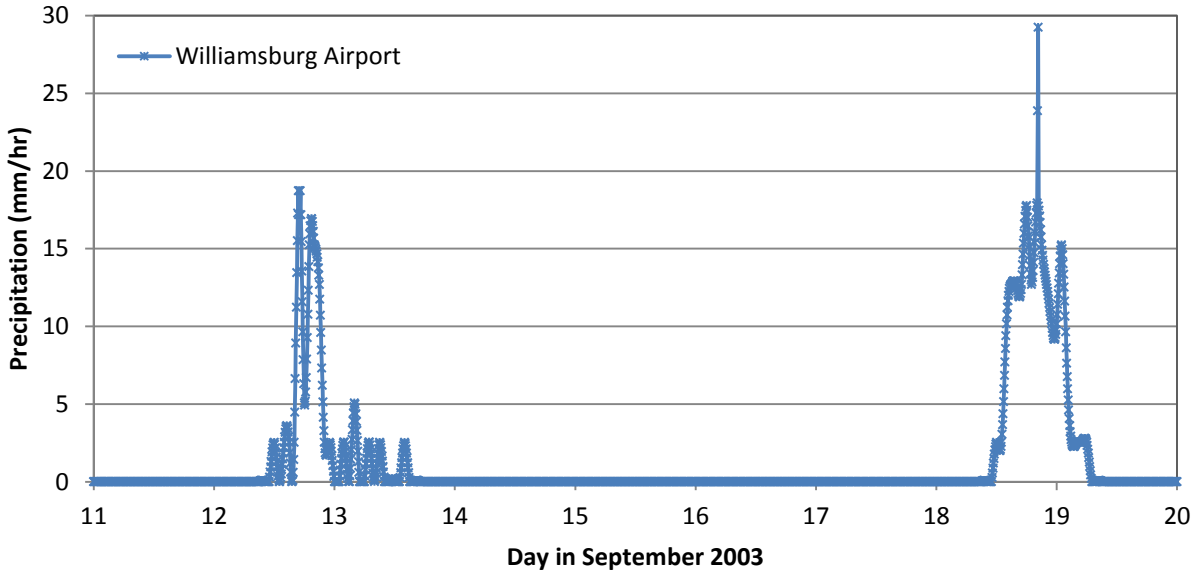

Figure 2.1. Precipitation input data for 2003 Hurricane Isabel from Williamsburg/Newport News Airport shown with a peak observed precipitation rate of 28 mm/hr on September 18, 2011, at 20:00 GMT.

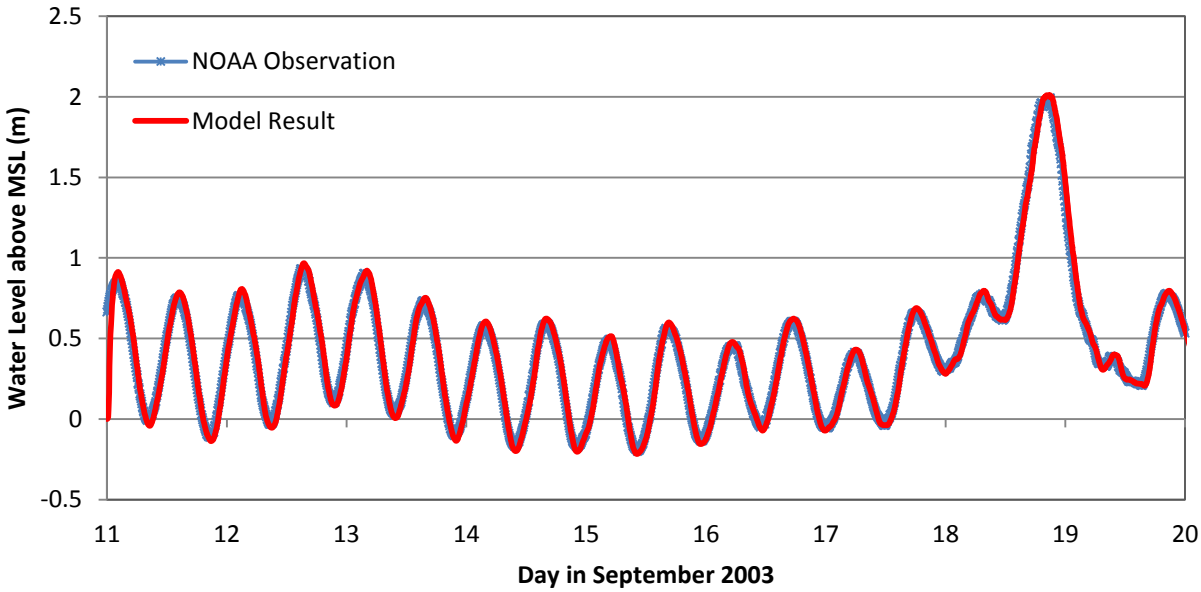

Figure 2.2. 2003 Hurricane Isabel temporal comparison in GMT of observed results (Sewells Point) and sub-grid results (R^2 = 0.9903) with an observed peak of 2.016m above mean sea level.

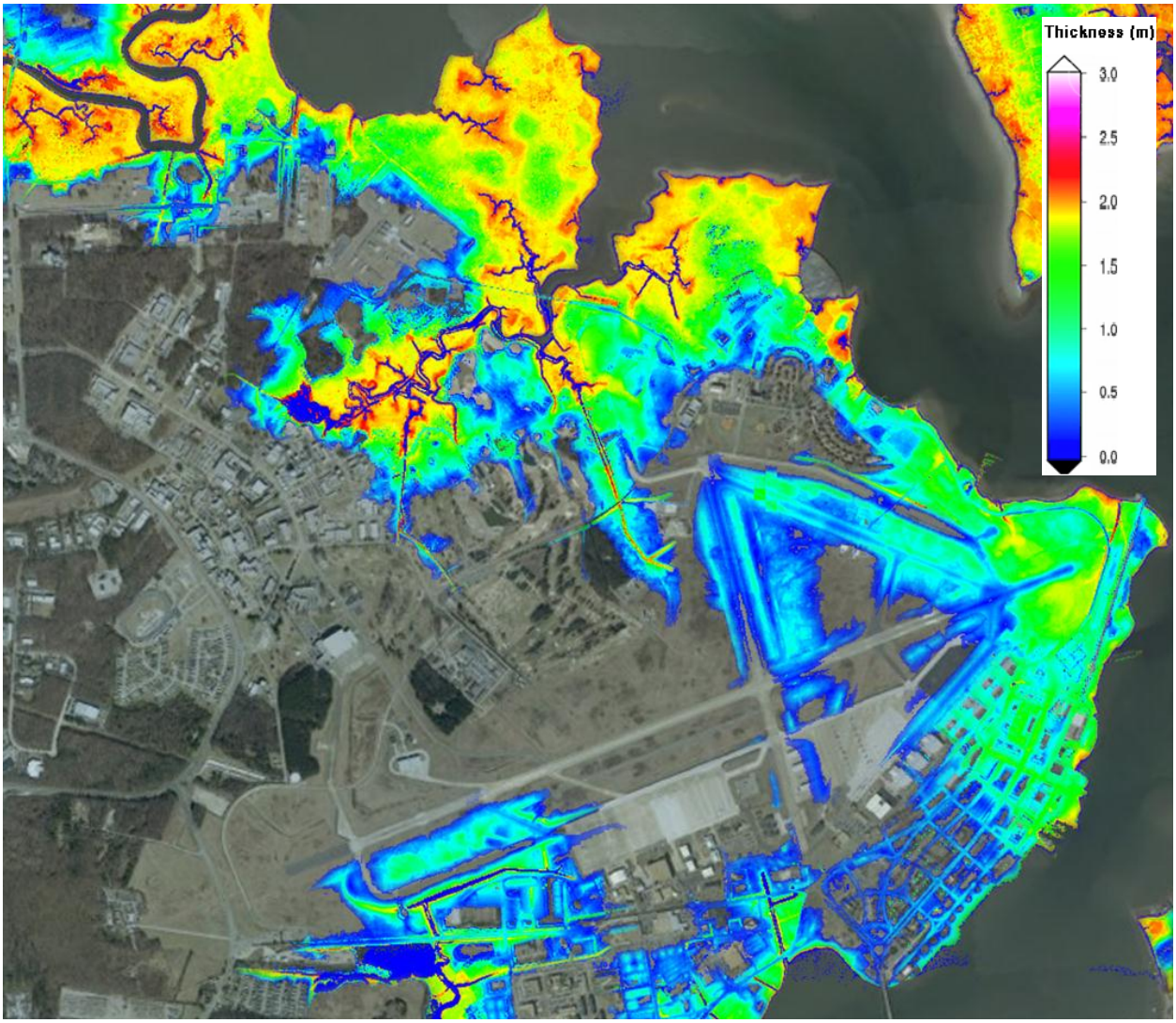

Figure 2.3A. Inundation thickness (height of water above the topographic land surface) map in meters for 2003 Hurricane Isabel without precipitation over the Back River peninsula with Langley Air Force Base in the south (lower) end and NASA Langley Research Center in the north (upper) end of the map.

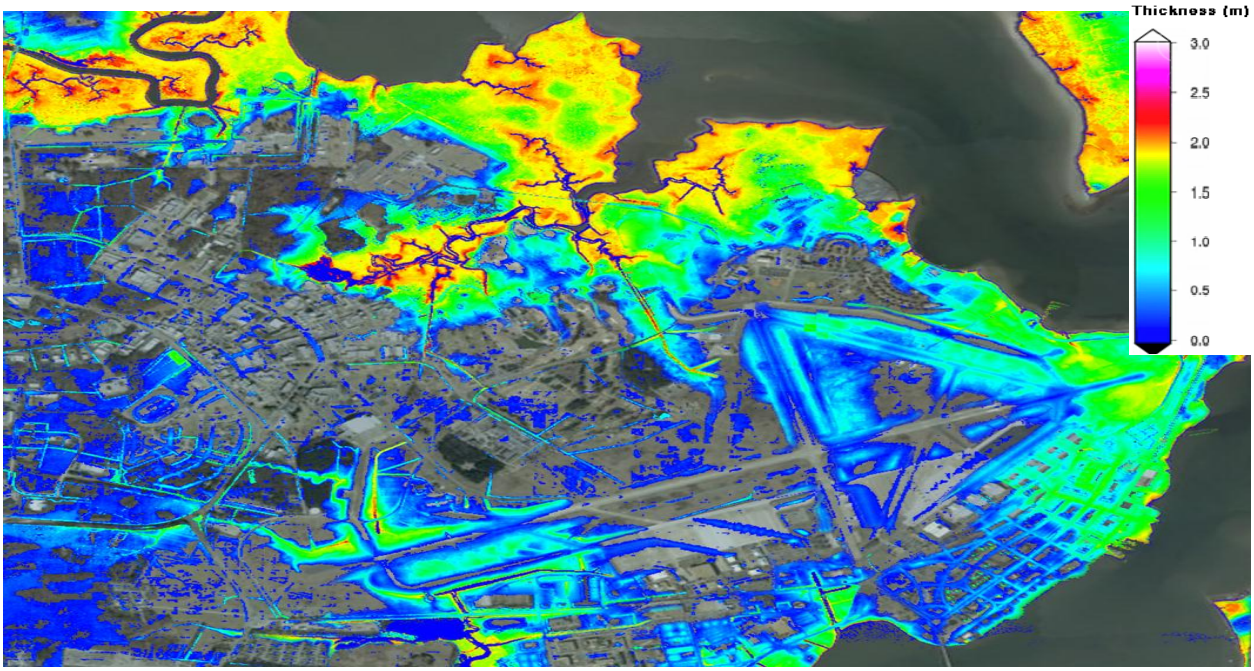

Figure 2.3B. Inundation thickness map in meters for 2003 Hurricane Isabel including precipitation input over the Back River peninsula with Langley Air Force Base in the south end and NASA Langley Research Center in the north (upper) end of the map.

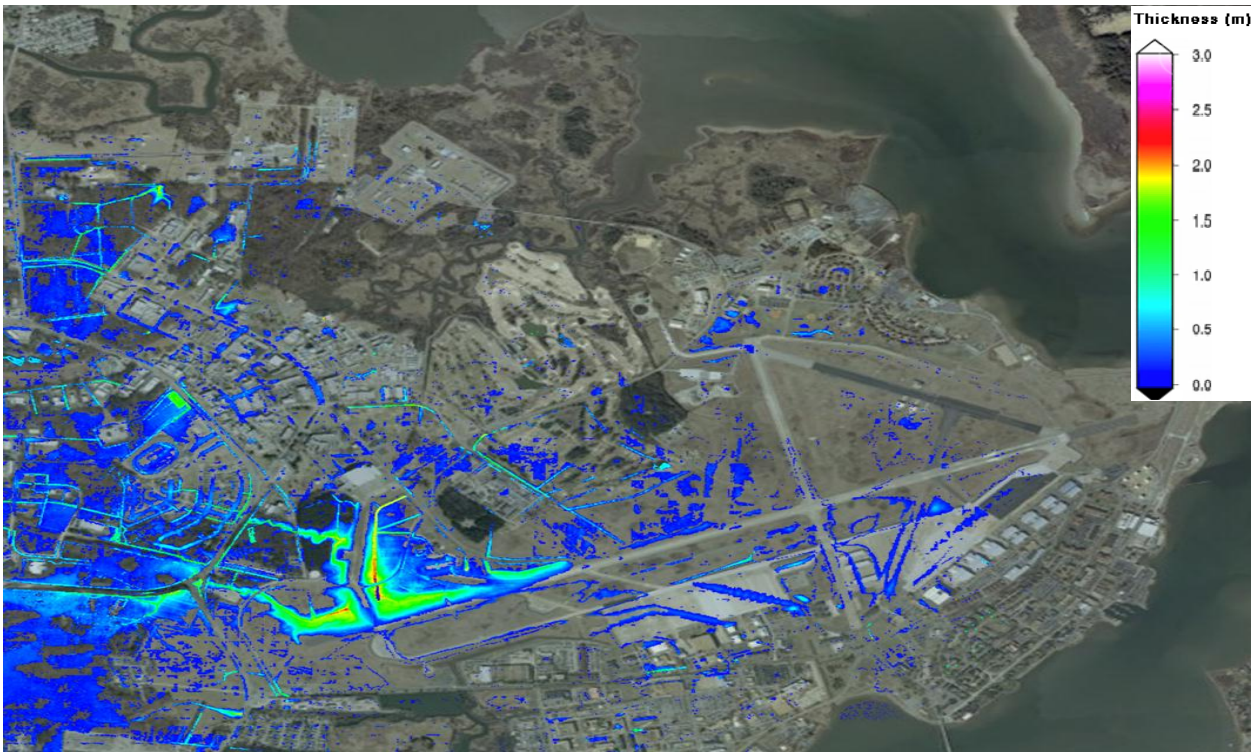

Figure 2.3C. Inundation difference map representing the influence of rainfall (Fig 2.3B – Fig. 2.3A) in meters by comparing Hurricane Isabel precipitation scenario to one without precipitation.

2.1.2 Climate Change Future Sea Level Rise Scenarios

Considering future sea level rise and climate change is important for coastal areas. To address these raising concerns, a series of sea level rise scenarios using the 2003 Hurricane Isabel model inundation as a base case (+00in) and then adding +15in, +30in, and +60in of future sea level rise were generated to observe the inundation result of this sea level rise at NASA Langley. In Figure 2.4, a time series of sea level rise scenarios describes the inundation peaks for the original storm (+00in) at 1.902m, Isabel +15in at 2.285m , Isabel +30in at 2.696m, and Isabel +60in at a maximum inundation of 3.460m . Spatial comparison maps of the four Hurricane Isabel sea level rise climate change scenarios are shown in Figure 2.5 A-D. The maximum inundation thickness is shown in the maps focused on the central region of NASA Langley Research Center as it backs up to a tidal tributary creek that feeds into the Back River estuary.

In the climate change scenarios, only storm surge flooding associated with sea level rise was utilized with no precipitation input, as it is impossible to accurately anticipate what the future precipitation rates would be with a future storm system of the magnitude of 2003 Hurricane Isabel (Figure 2.5A) at Isabel +15in (Figure 2.5B), Isabel +30in (Figure 2.5C), and Isabel +60in (Figure 2.5D). Also, the desire in this simulated series is to assess the inundation threat posed via future sea level rise associated with climate change, and neglecting precipitation allows the maximum inundation maps to more clearly reflect the storm surge-induced flooding associated with increasing sea level.

2.2 Results for 2011 Hurricane Irene

2.2.1 Storm Tide Comparison

A peak precipitation rate of 46 mm/hr was observed at the Williamsburg/Newport News Airport during 2011 Hurricane Irene on August 28, 2011, at 05:00 GMT as shown in Figure 2.6. A temporal comparison of observed results at Langley Tide Gauge 1 and sub-grid results using the Back River Dandy Haven VIMS TideWatch observation data for 2011 Hurricane Irene yields a correlation of $R^2 = 0.9714$ ($R^2 = 0.9486$ around the three day peak) with an observed maximum inundation peak of 1.656m above mean sea level as shown in Figure 2.7.

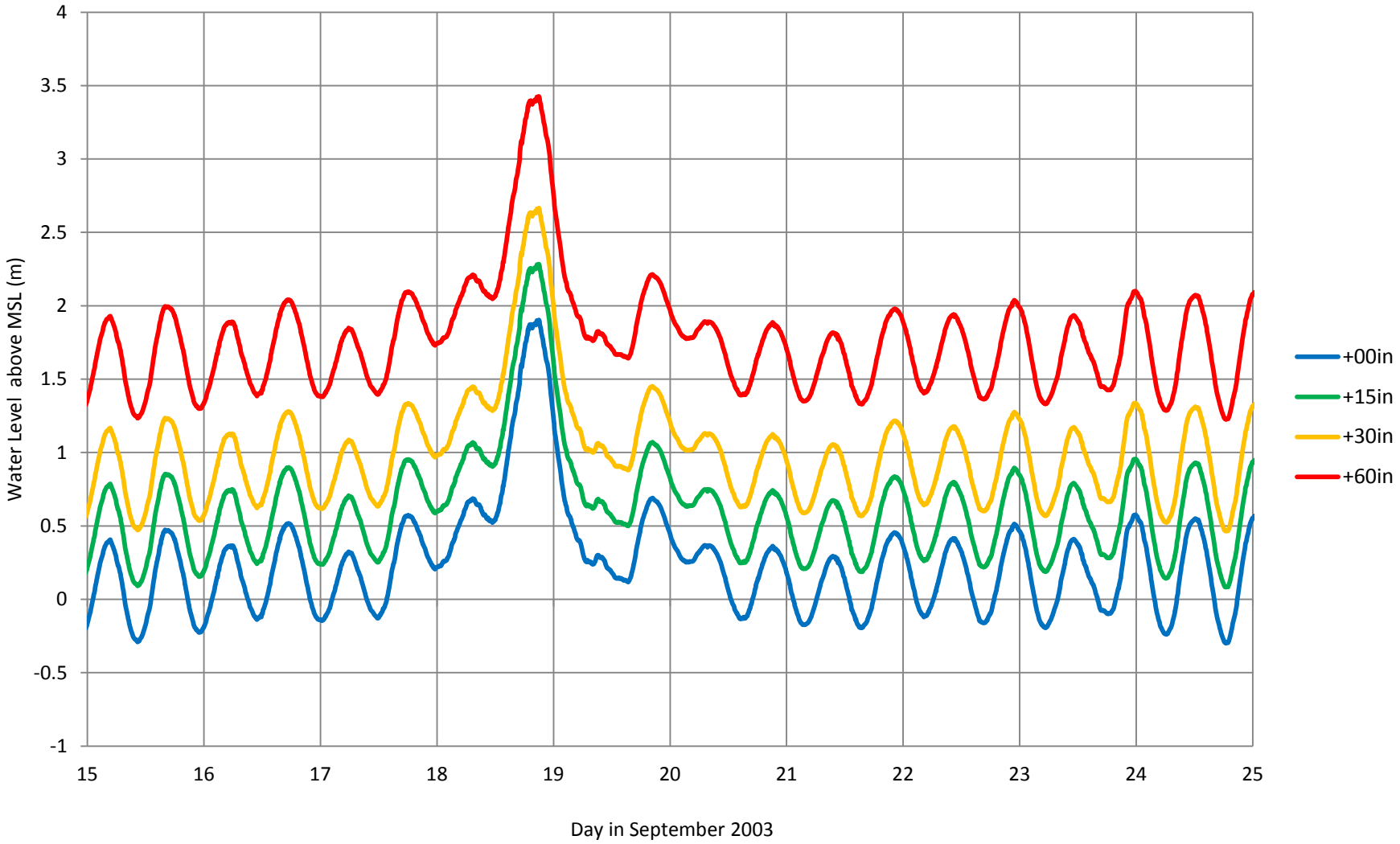

Figure 2.4. Time series of elevation forcing at the open boundary for four 2003 Hurricane Isabel sea level rise scenarios including the original storm at +00in, +15in, +30in, and +60in.

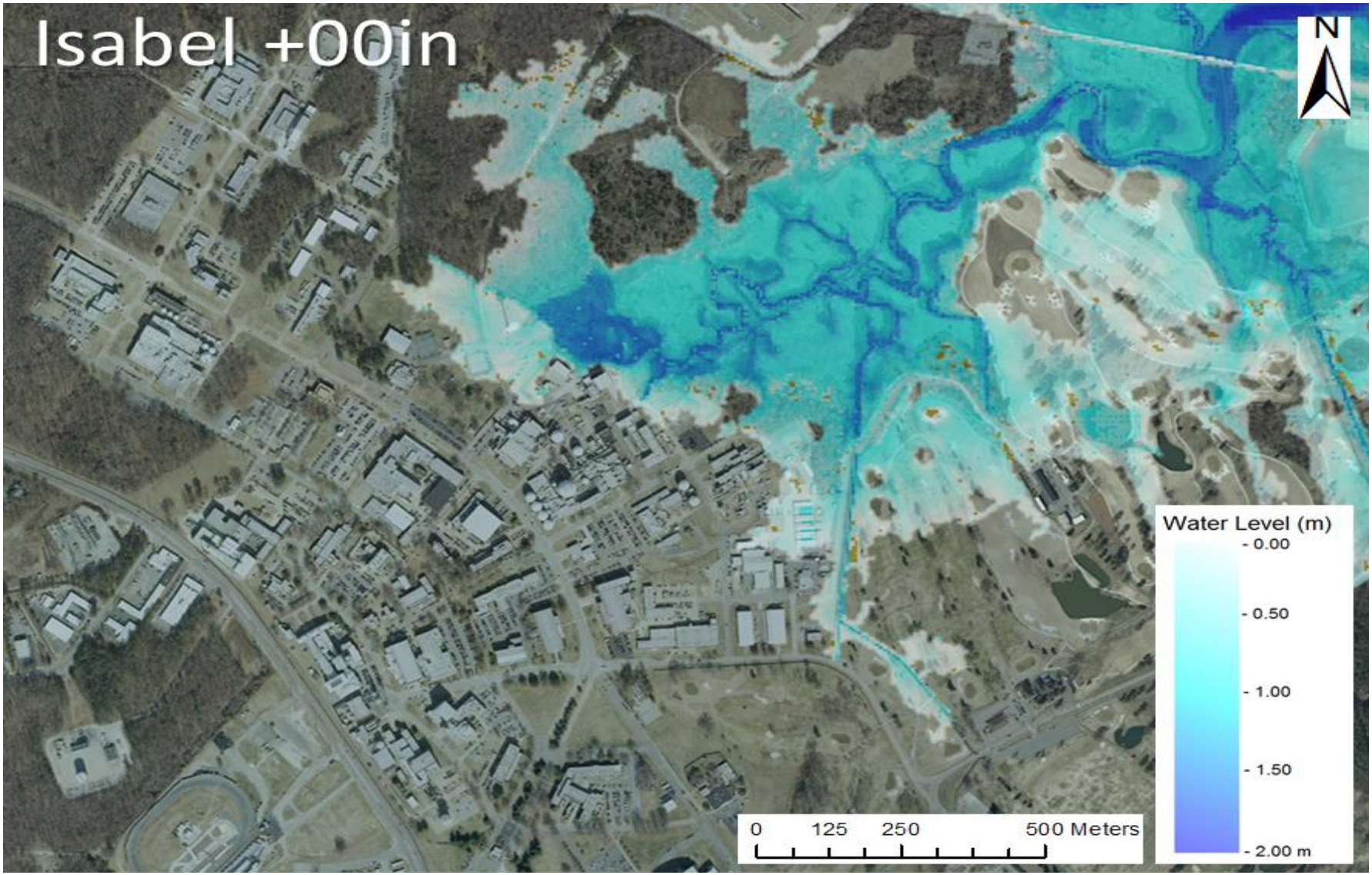

Figure 2.5A. 2003 Hurricane Isabel inundation with +00in sea level rise added scenario in the central region of NASA Langley. The emphasis is on the inundation extent as a function of future sea level rise.

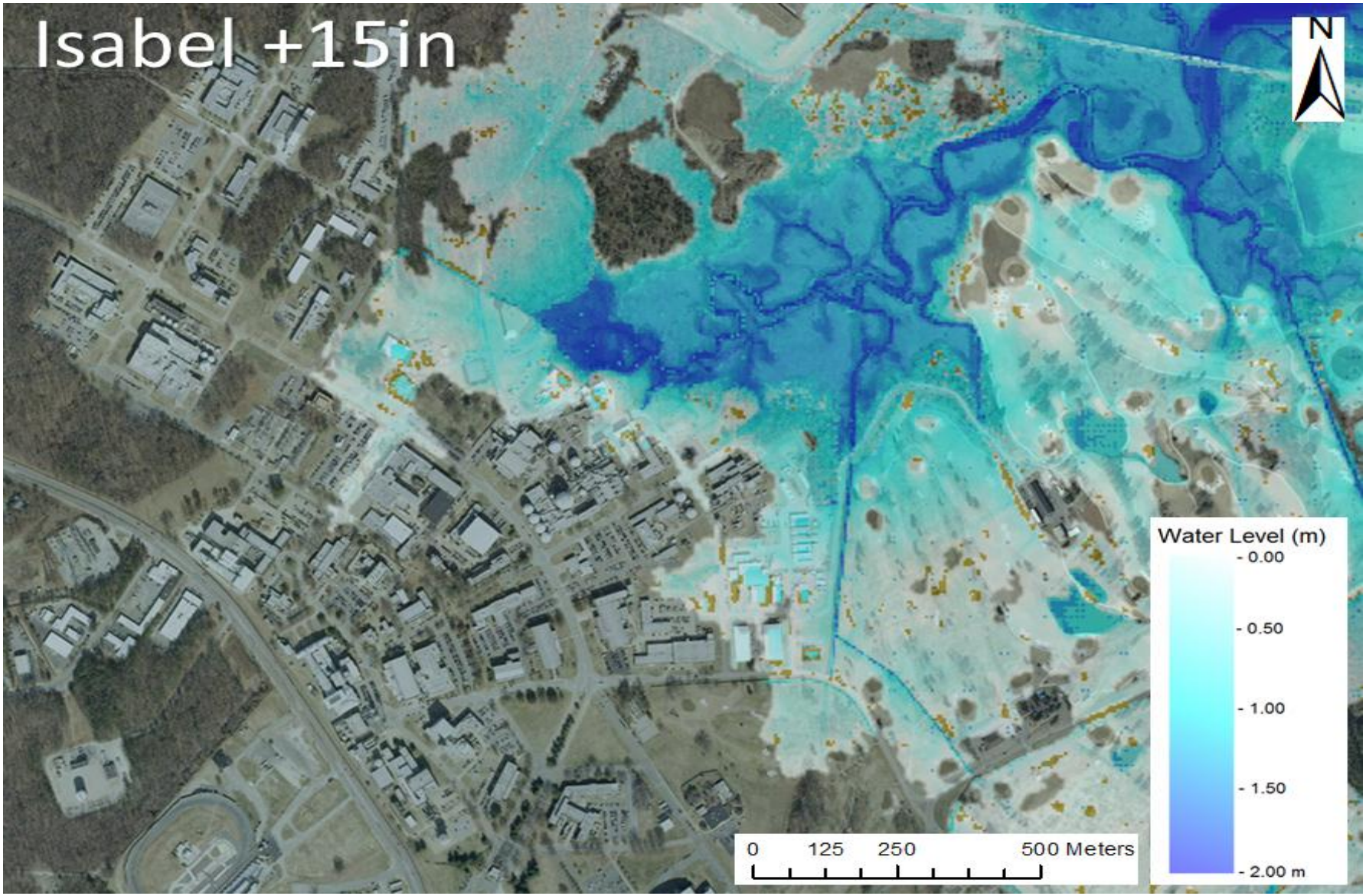

Figure 2.5B. 2003 Hurricane Isabel sea level rise climate change scenario for Isabel +15in in the central region of NASA Langley.

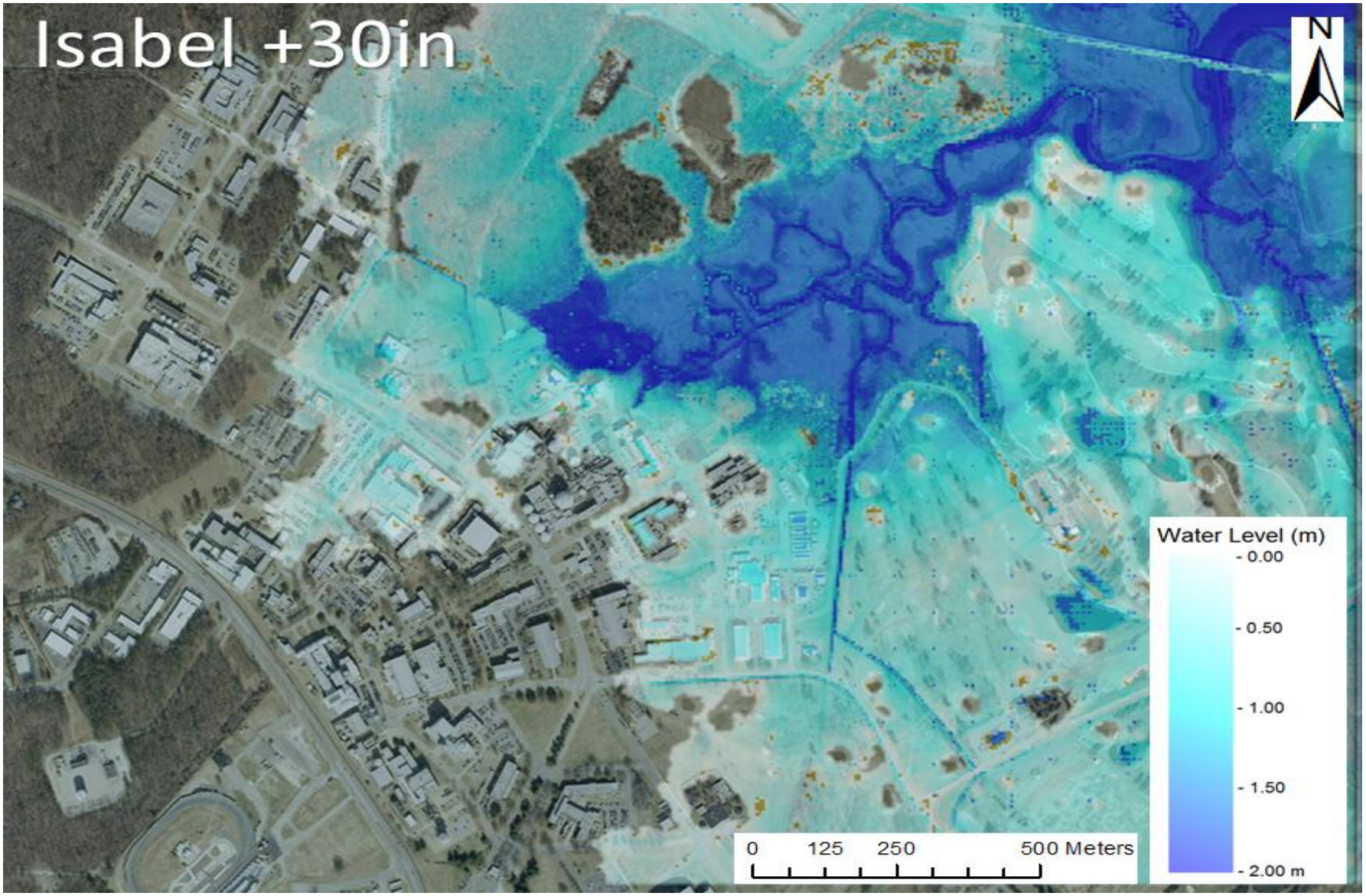

Figure 2.5C. 2003 Hurricane Isabel sea level rise climate change scenario for Isabel +30in in the central region of NASA Langley.

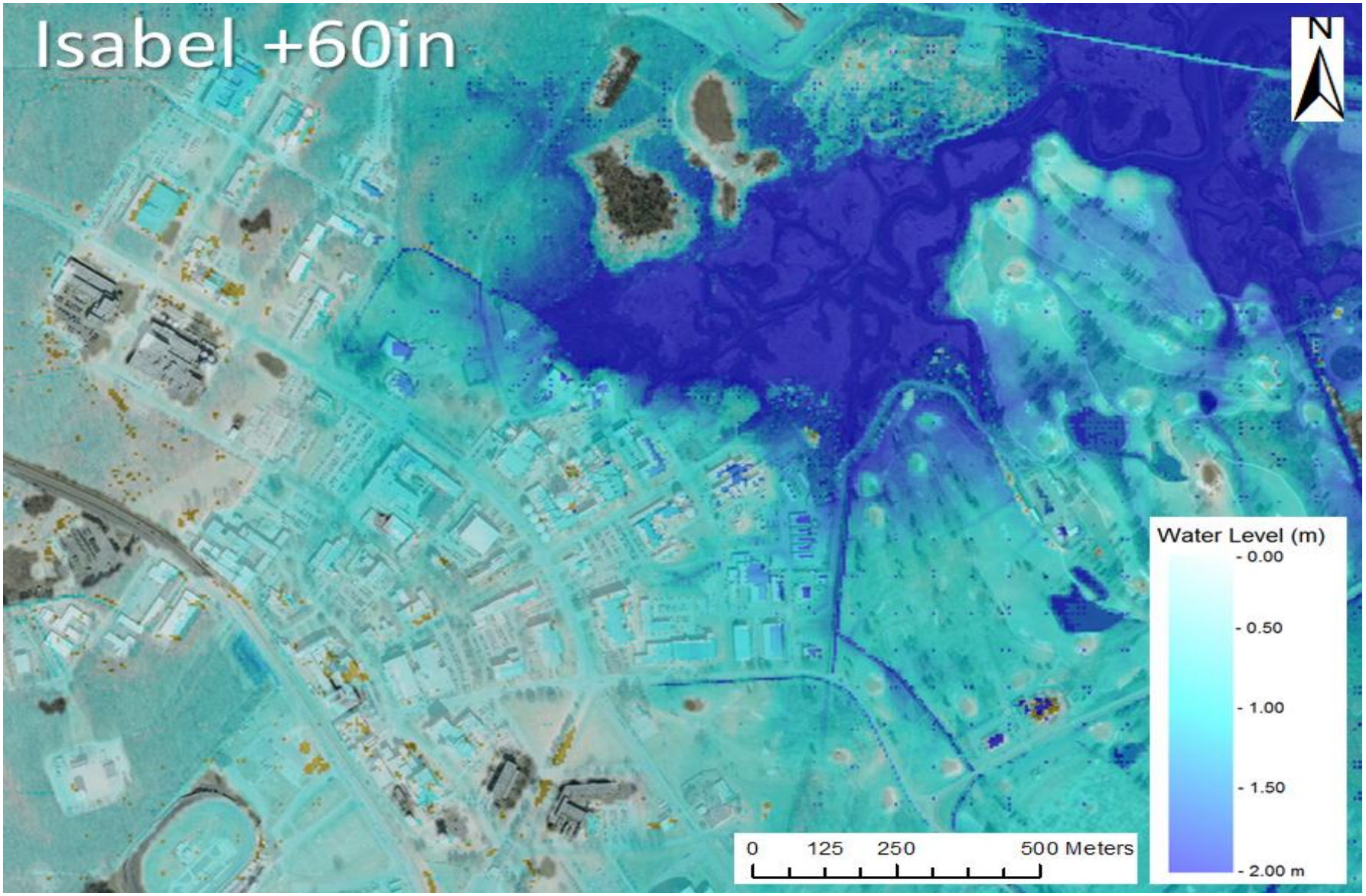

Figure 2.5D. 2003 Hurricane Isabel sea level rise climate change scenario for Isabel +60in in the central region of NASA Langley.

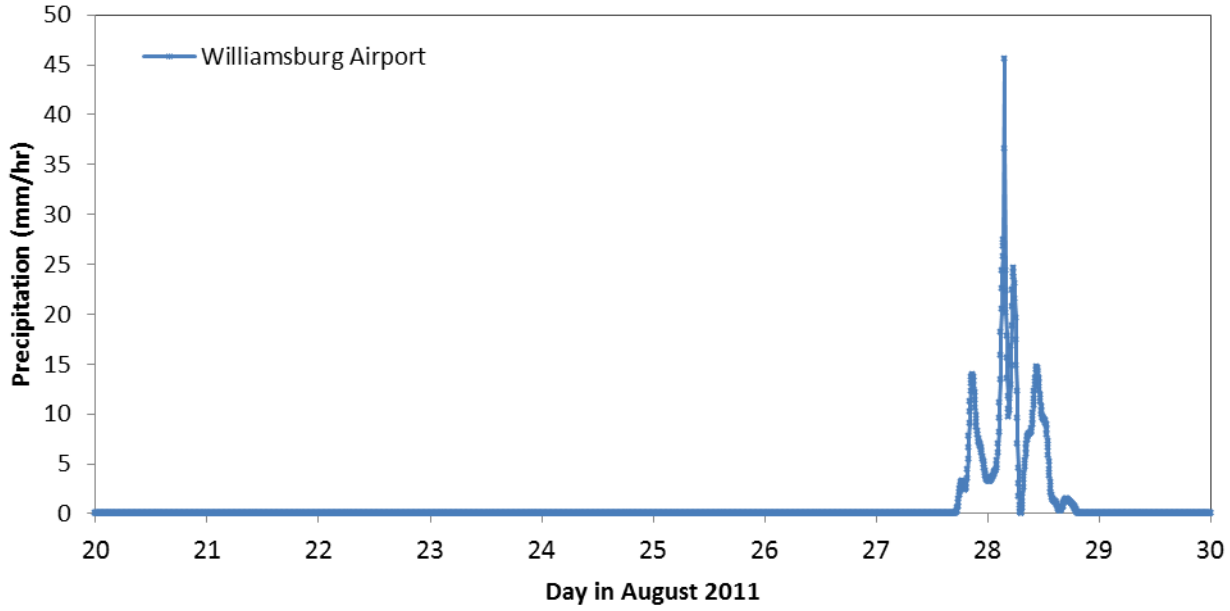

Figure 2.6. Precipitation input data from Williamsburg/Newport News Airport shown for 2011 Hurricane Irene with a peak observed precipitation rate of 46 mm/hr August 28, 2011, at 05:00 GMT.

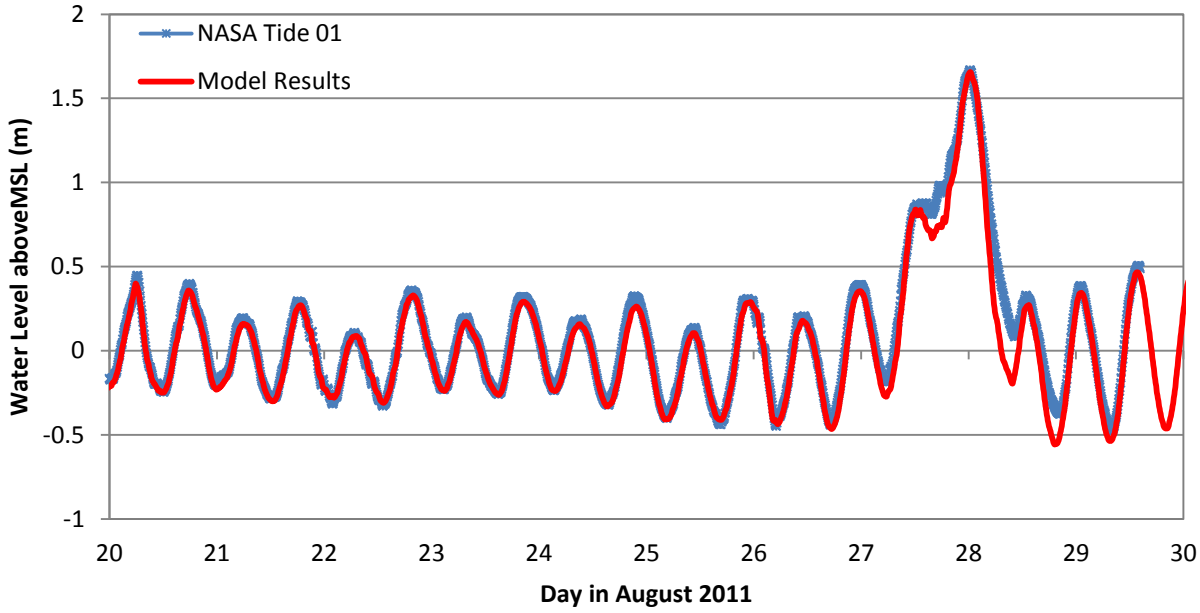

Figure 2.7. 2011 Hurricane Irene temporal comparison in GMT of observed results (NASA Tide 01) and sub-grid results (R^2 = 0.9714 and R^2 = 0.9486 for three days around peak) with an observed peak of 1.656m above mean sea level.

2.2.2 Wrack Line Comparison

A wrack line vertical inundation comparison was performed utilizing the NASA-collected debris data collected from the aftermath of 2011 Hurricane Irene at six flooded sites as shown in Figure 2.8. These deposited debris lines were utilized as a proxy for comparison of sub-grid model results for maximum extent of inundation as an additional metric for evaluating the accuracy of the sub-grid model's predicted spatial inundation on a 5m sub-grid. Water level thickness will be calculated via maximum water level elevation (maximum water surface level) - the sub-grid topography elevations at each recorded GPS wrack line point using GIS to retrieve the model-computed thickness at each wrack line point. Ideally, this value should be close to 0m for a perfect match, although with the precipitation input, we do not exactly know how much water was infiltrated through the soil. Additionally, the buildings shown in Figures 2.9A-F have been filtered out of the Lidar topography data and are not present in the model sub-grid results. Provided accurate building heights, buildings may be assessed in future model simulations for integration with the Lidar-derived sub-grid topography.

Site A is located near the tidal tributary to the Back River estuary in the central region of Langley near buildings 1256 and 1247 as shown in Figure 2.9A. The wrack line contains 35 points with a localized maximum observed water level of 1.802m with an average difference/water thickness of 0.128m (without infiltration) and 0.052m with 10% infiltration is considered as shown in Table B1 (Appendix B).

The wrack line at Site B is also located near the tidal tributary to the Back River estuary in the central region of Langley west of Site A near buildings 1222 and 1223 as shown in Figure 2.9B. This wrack line consists of 25 different recorded points with a local maximum water level of 1.801m with an average difference/water thickness of 0.110m (without infiltration) and 0.070m with 10% infiltration is considered as shown in Table B2 (Appendix B).

Site C's wrack line is populated with 32 GPS points located adjacent to Back River in the north end of NASA Langley Research Center near building 1275 as shown in Figure 2.9C. The wrack line is positioned at a location where the maximum water level is 1.766m with an average difference/water thickness of 0.167m (without infiltration) and 0.010m with 10% infiltration is considered as shown in Table B3 (Appendix B).

Site D is the shortest wrack line consisting of 4 GPS data points located near a meandering tidal creek connecting the Big Bethel Reservoir to the Back River estuary in the north end of Langley near buildings 1158 and 1159 as shown in Figure 2.9D. The maximum water level is 1.780m at the wrack line where an average difference/water thickness of 0.227m (without infiltration) and 0.049m with 10% infiltration is considered was calculated as shown in Table B4 (Appendix B).

The wrack line measured at Site E is also located adjacent to the meandering tidal creek connecting the Big Bethel Reservoir to the Back River estuary close to the location of the Langley Tide Gauge 1 in the north end of Langley southwest of Site D near building 1196 adjacent to a drainage creek running nearly parallel to building 1257 as shown in Figure 2.9E. This wrack line consists of 14 different recorded points with a local maximum water level of

1.780m with an average difference/water thickness of 0.231m (without any infiltration) and 0.053m with 10% infiltration is considered as shown in Table B5 (Appendix B).

Site F is located west of Site E also located parallel to the west end of building 1257 adjacent to the meandering tidal creek on the north end of Langley near building 1258 as shown in Figure 2.9F. The wrack line contains 7 points with a localized maximum observed water level of 1.802m with an average difference/water thickness of 0.168 (without any infiltration) and 0.011m with 10% infiltration is considered as shown in Table B6 (Appendix B). Site F has the best horizontal maximum inundation comparison following the wrack line within 2.5m, followed closely by Site E (6.5m), and then site A (8.5m).

All of the sites fit within two sub-grid cells' length in distance (on average) for inundation thicknesses greater than 0.05m from the GPS-recorded wrack line data. For the sites with larger horizontal distances from their GPS-recorded wrack lines, these sites are located in very flat areas where much of the horizontal discrepancy is attributed to precipitation-induced inundation on the order of <0.05m. In terms of vertical maximum inundation differences with 10% infiltration, Site C ranked the best with a difference of 0.010m, followed closely by the wrack line at Site F with a measured difference of 0.011m.

In summary, the wrack line measurements at NASA Langley Research Center provide a unique observation dataset that can be utilized to assess the maximum extent of the inundation during a storm event. The maximum water level computed from the model compared favorably with the local topography (in m above NAVD88) within 10% of error if infiltration is assumed to be 0 and the error is within 2-5% error if 10% infiltration is considered. This assessment is consistent with the rational C factor approach assuming that the infiltration is constant:

$$Q = C \times I \times A$$

Where Q is the peak runoff value, I is the average rainfall intensity, A is the drainage area and C is the runoff coefficient ranging from 0.1 to 0.9 depend on the land use, soil type and soil condition.

Figure 2.8. GPS wrack line/debris locations for observation data collected by NASA Langley Research Center immediately after 2011 Hurricane Irene.

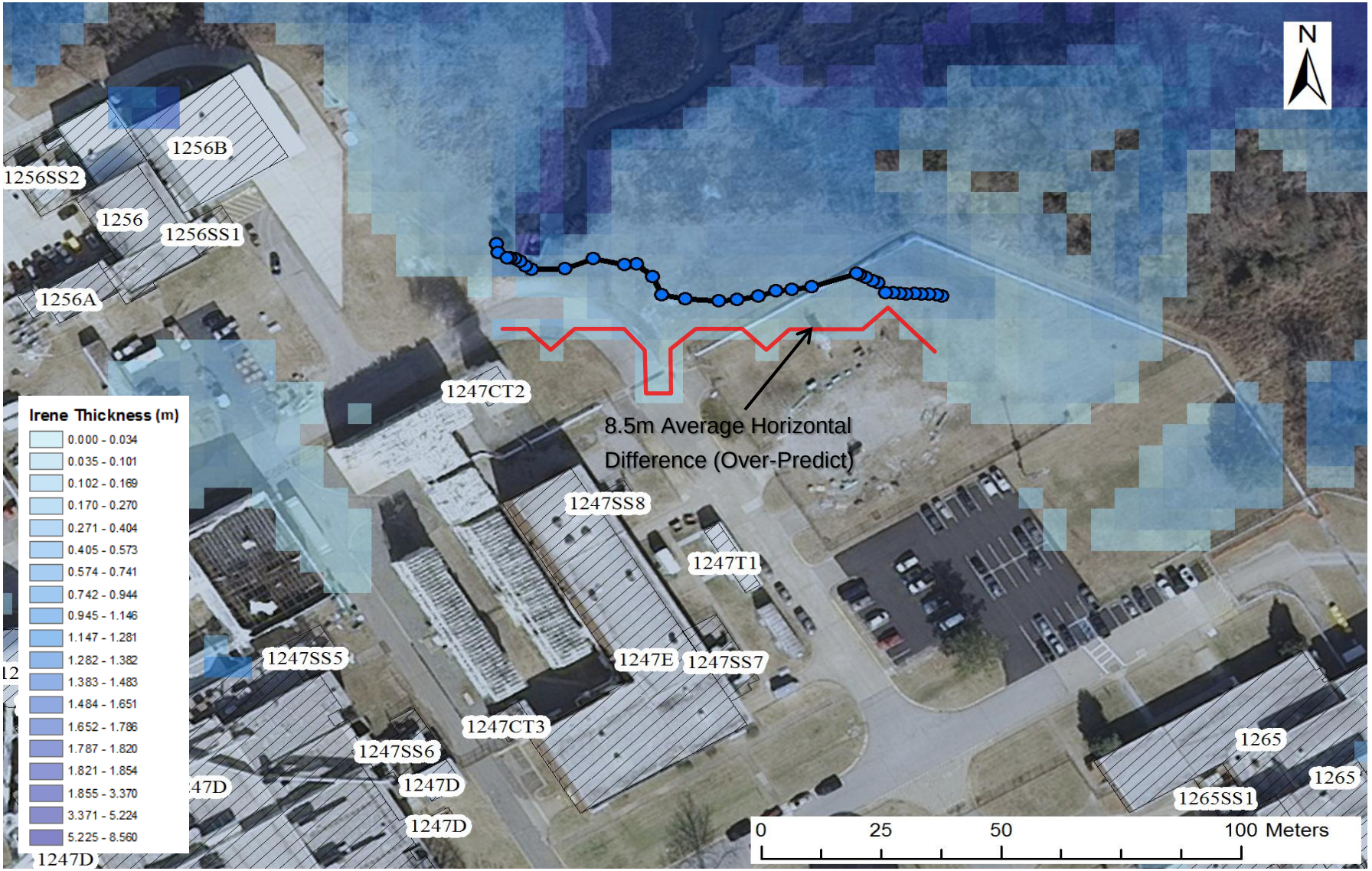

Figure 2.9A. Spatial comparison of maximum extent of inundation for 2011 Hurricane Irene at NASA Langley Research Center with GPS-recorded wrack line area A with depths corresponding with wrack line thicknesses in Table B1 (**blue dots**).

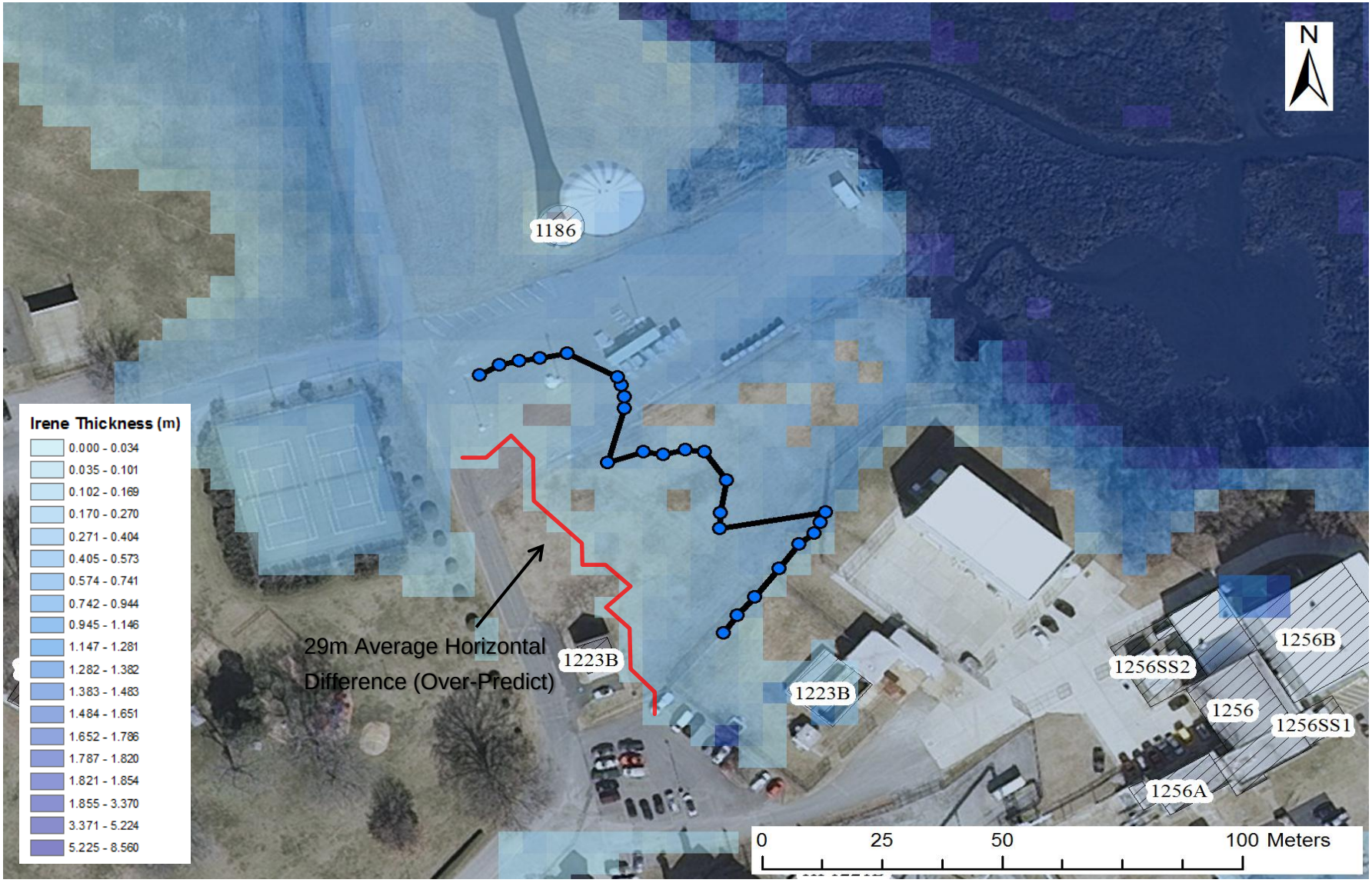

Figure 2.9B. Spatial comparison of maximum extent of inundation for 2011 Hurricane Irene at NASA Langley Research Center with GPS-recorded wrack line area A with depths corresponding with wrack line thicknesses in Table B2 (**blue dots**).

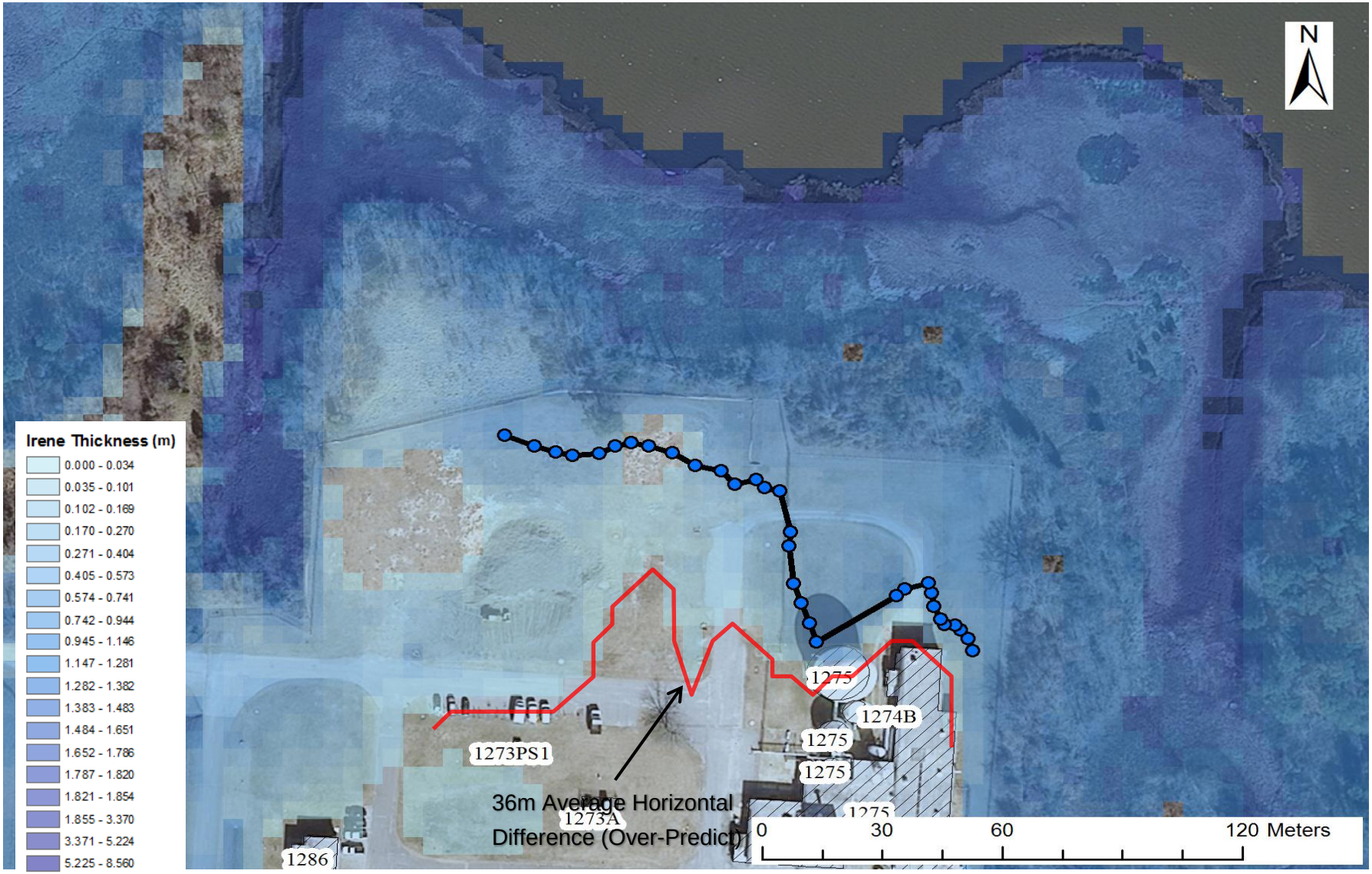

Figure 2.9C. Spatial comparison of maximum extent of inundation for 2011 Hurricane Irene at NASA Langley Research Center with GPS-recorded wrack line area A with depths corresponding with wrack line thicknesses in Table B3 (**blue dots**).

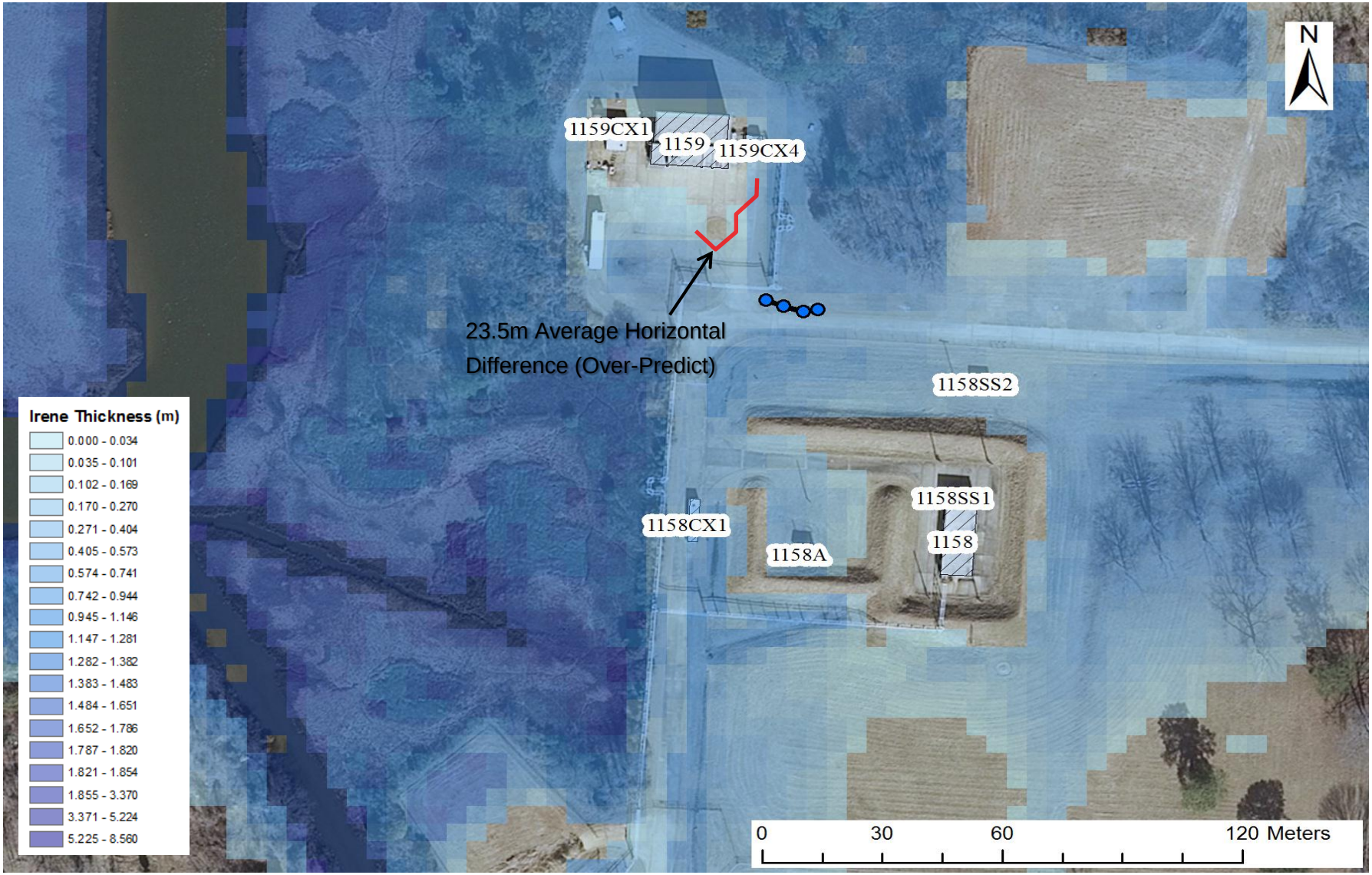

Figure 2.9D. Spatial comparison of maximum extent of inundation for 2011 Hurricane Irene at NASA Langley Research Center with GPS-recorded wrack line area A with depths corresponding with wrack line thicknesses in Table B4 (**blue dots**).

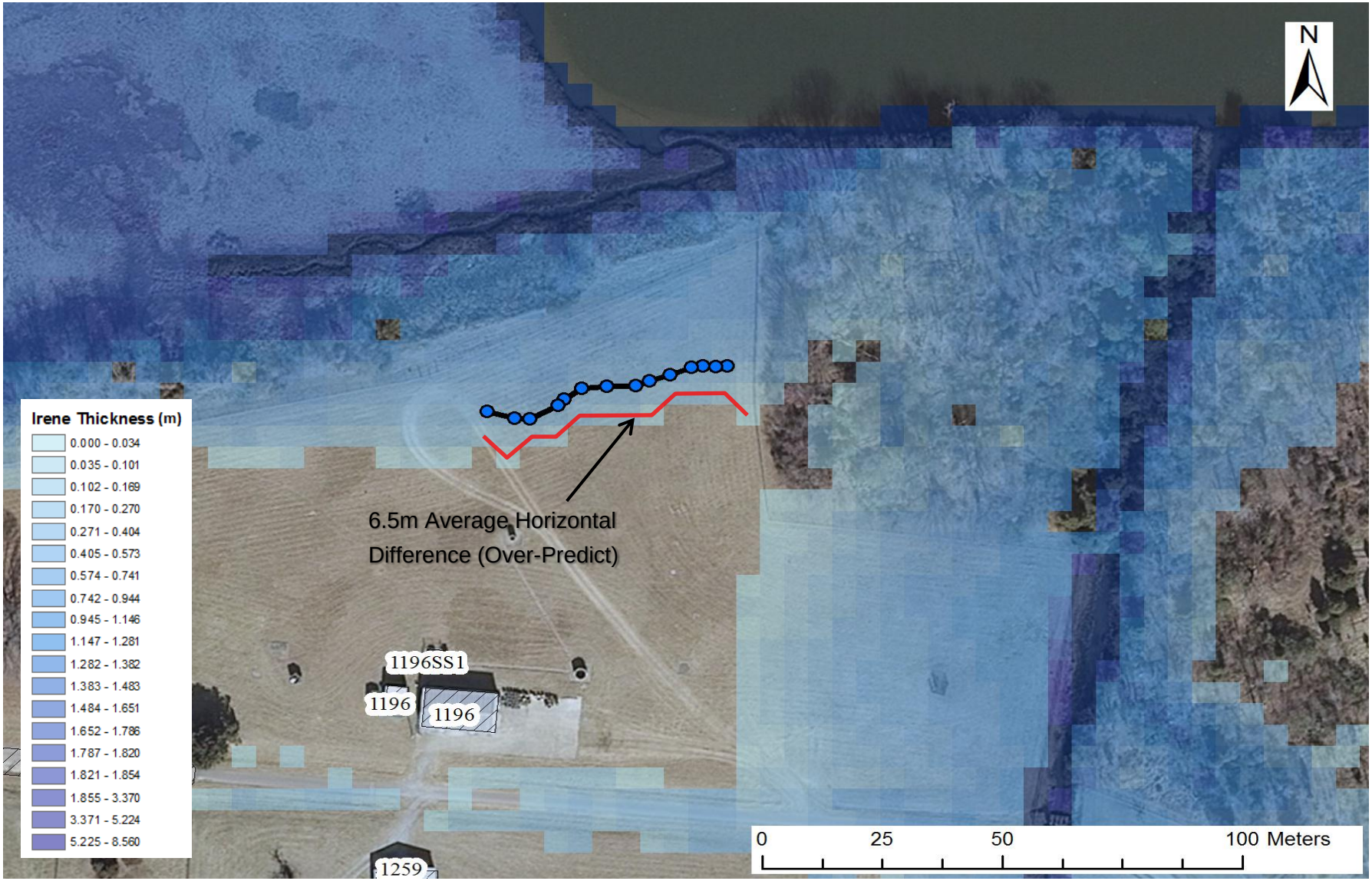

Figure 2.9E. Spatial comparison of maximum extent of inundation for 2011 Hurricane Irene at NASA Langley Research Center with GPS-recorded wrack line area A with depths corresponding with wrack line thicknesses in Table B5 (**blue dots**).

Figure 2.9F. Spatial comparison of maximum extent of inundation for 2011 Hurricane Irene at NASA Langley Research Center with GPS-recorded wrack line area A with depths corresponding with wrack line thicknesses in Table B6 (**blue dots)**.

3. Discussion and Conclusion

3.1 Discussion

One of the main assumptions of this study is that the ground is completely saturated and therefore there is not water infiltration. In practice, rainfall reaching the land surface can infiltrate into the pervious soil. Soil has a finite capacity to absorb water. The infiltration capacity varies not only from soil to soil, but is also different for dry versus moist conditions based upon the hydraulic conductivity gradient in the same soil. Upon consideration of soil infiltration rates, a runoff coefficient can range from 0.1 to 0.9. Thus, the inundation prediction without infiltration represents the most conservative (worst case scenario) estimation of the flooding which can occur given the observed amount of precipitation.

If fluid is allowed to permeate through the model grid, the degree of over-prediction associated with the precipitation input from the model may be appropriately balanced. Preliminary tests employing a spatially-varying infiltration rate have shown marked improvement in wrack line comparison results. Provided a spatially-varying infiltration rate assigned according to the varying degrees of impervious nature of different land cover classifications from the National Land Cover Database (via percentage of land cover with vegetation available for absorbing flood waters and precipitation after a storm has passed), higher percentages of land cover with vegetation equates to a greater absorption into the soil, and a higher infiltration rate (Figure 3.1). In likewise fashion, less vegetation and greater percentages of urban infrastructure including paved surfaces (streets, some drainage structure, and runways) equates to more impervious surfaces for a lower infiltration rate. Land cover data were utilized in GIS as a proxy to specify flags in the model's Fortran code corresponding with the areas shown in the model grid with an example shown in Figure 3.2, translating to improved horizontal (Figure 3.3A–B) and vertical (Table 3A–B) wrack line results comparisons.

Incorporation of land use classifications as a proxy for spatially-varying infiltration rates in the sub-grid model results in the wrack line at Site E (near the location of the NASA Tide 01 tide gauge in an estuarine emergent wetland classification area in Figure 3.3A) yields a decrease of 0.084m for a water thickness of 0.147m (± 0.035m standard deviation) as shown in Table 3A. Site F is also adjacent to an estuarine emergent wetland classified area, and incorporation of spatially-varying infiltration results in a decrease of 0.064m for a water thickness of 0.103m (± 0.049m standard deviation) as shown in Table 3B. Spatially-varying infiltration rates may be further addressed in a phase II portion of this project and may better constrain the effect of the precipitation input utilized in the sub-grid model, thus further improving upon the wrack line comparison results.

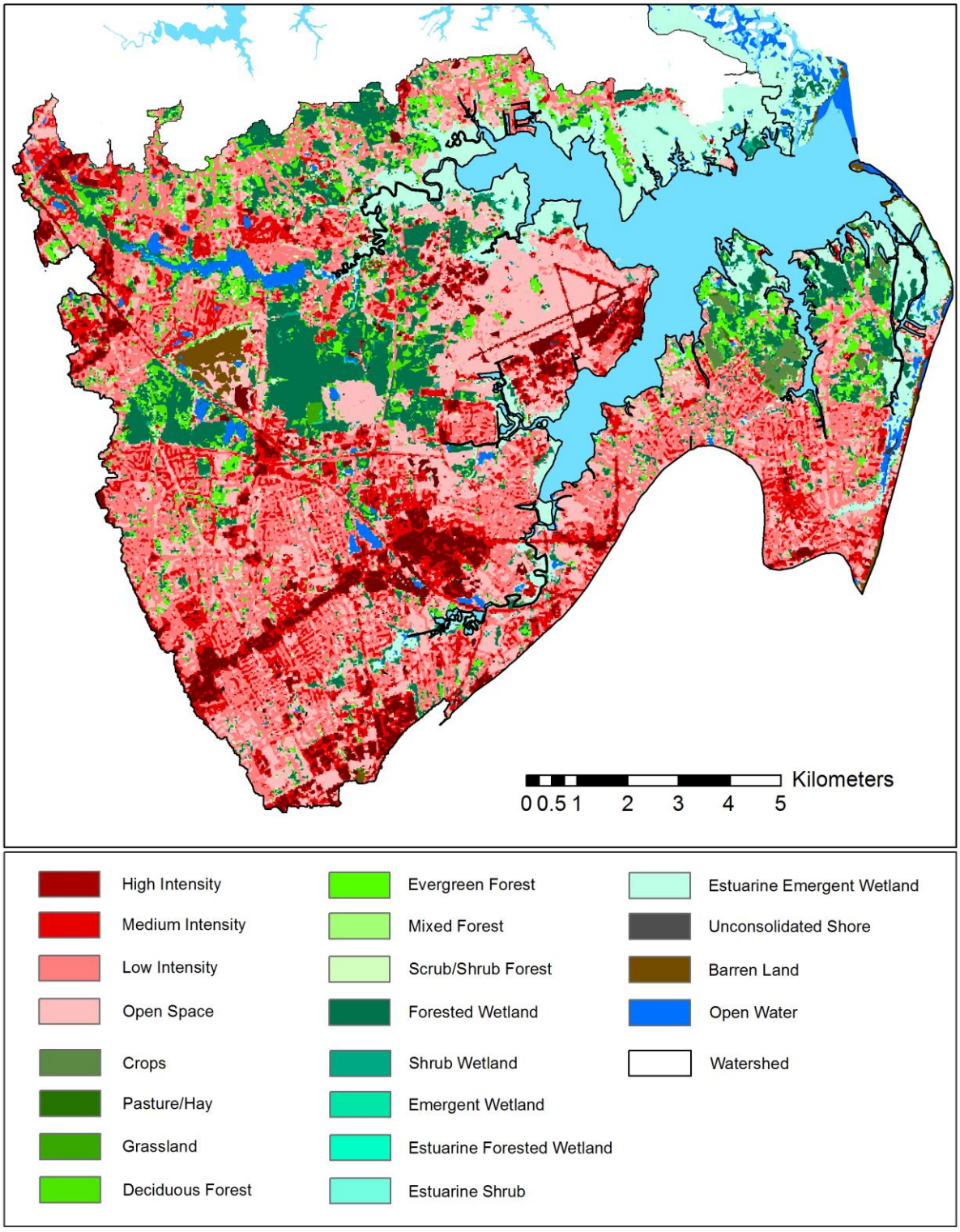

Figure 3.1. Land use map for the Back River watershed with developed land shown in red hues and vegetated land displayed with green hues with north at top (Source: National Land Cover Database, 2006).

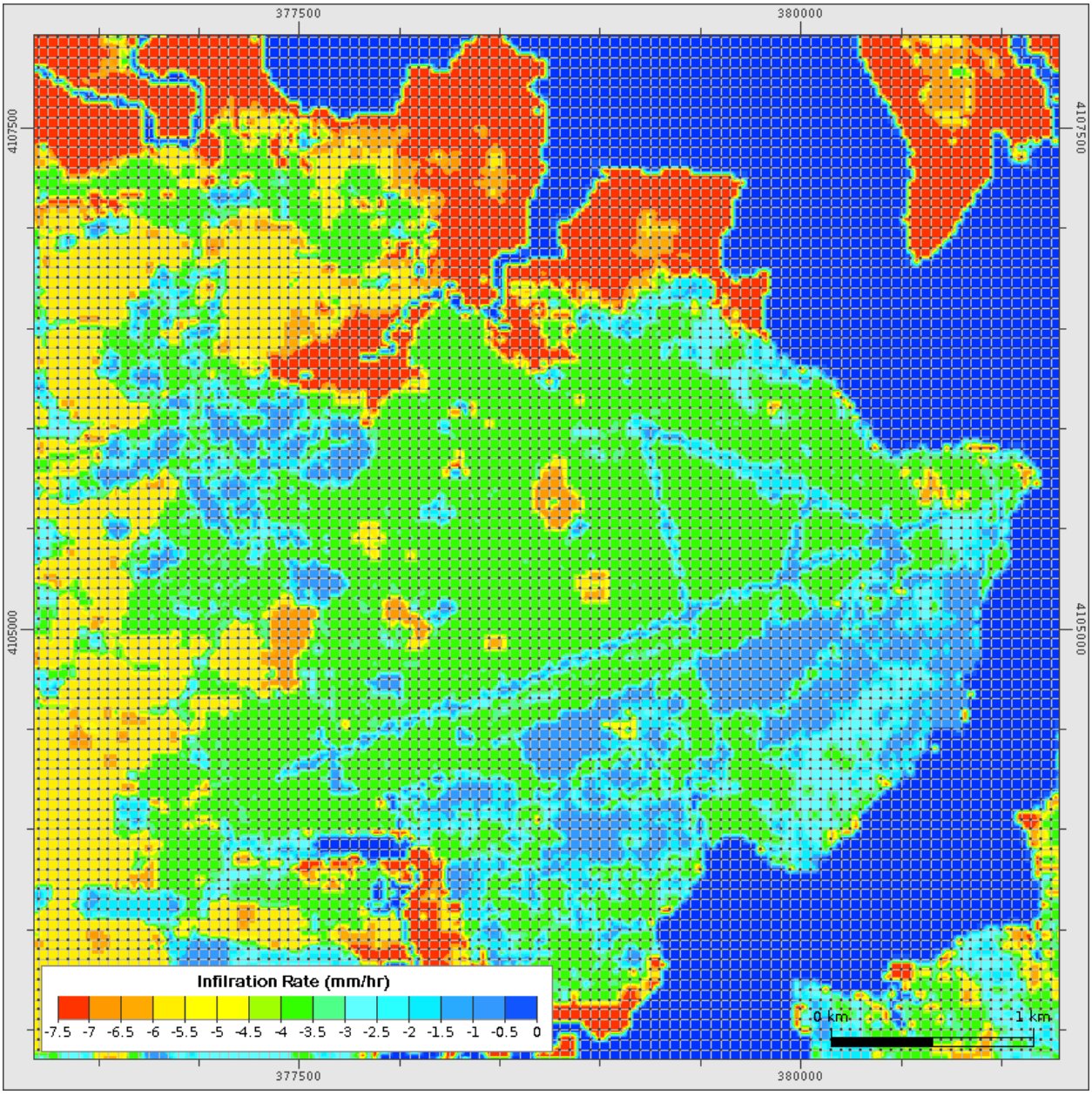

Figure 3.2. Example of a spatially-varying infiltration rate in mm/hr for NASA Langley Research Center and Langley Air Force Base using 30m-resolution land use data with 50m base grid cells and 5m sub-grid cells illustrated.

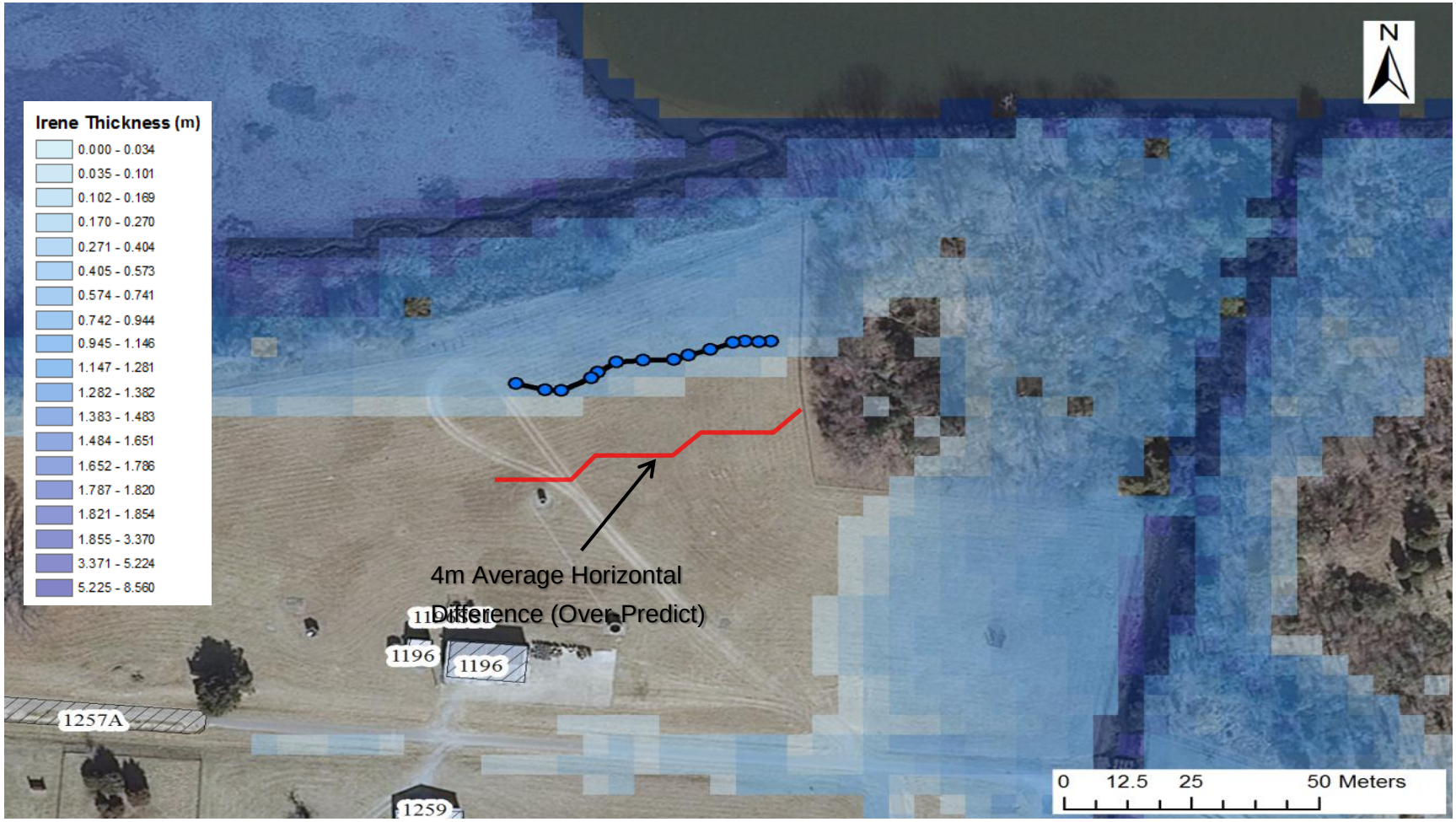

Figure 3.3A. Spatial comparison of maximum extent of inundation for 2011 Hurricane Irene at NASA Langley Research Center with GPS-recorded wrack line at Site E with depths corresponding with wrack line thicknesses in Table 3A (**blue dots**).

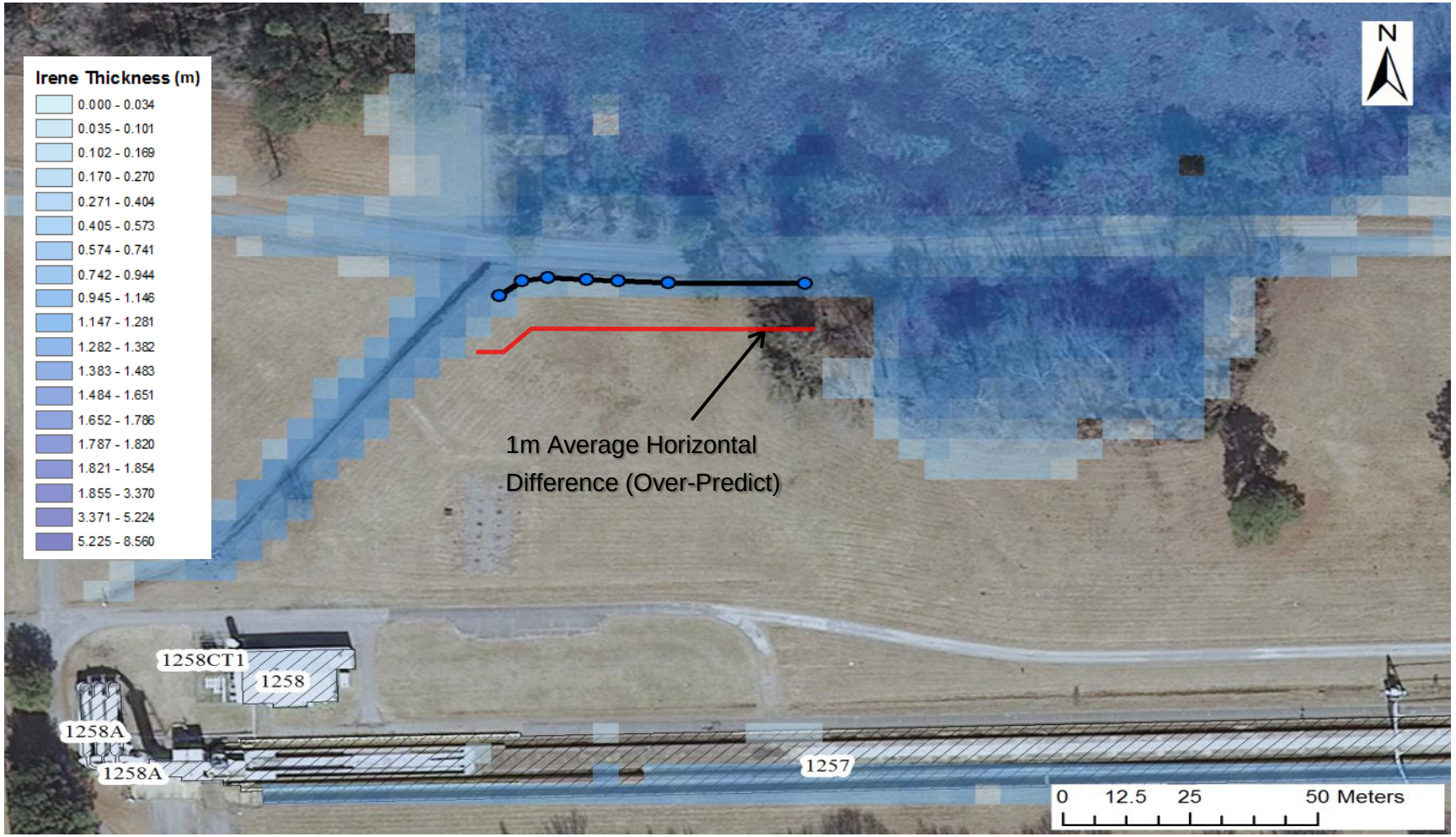

Figure 3.3B. Spatial comparison of maximum extent of inundation for 2011 Hurricane Irene at NASA Langley Research Center with GPS-recorded wrack line at Site F with depths corresponding with wrack line thicknesses in Table 3B (**blue dots**).

#	Wrack Line Point	Northing	Easting	Elevation (m)	Max Water Level without Infiltration (m)	Difference (m)	Max Water Level with SV Infiltration (m)	Difference with SV Infiltration (m)
1	VX558	1087664.55	3687772.84	1.531	1.780	0.249	1.696	0.165
2	VX559	1087663.20	3687778.58	1.594	1.780	0.186	1.696	0.102
3	VX560	1087663.25	3687781.84	1.618	1.780	0.162	1.696	0.078
4	a5062	1087666.59	3687787.50	1.554	1.780	0.226	1.696	0.142
5	a5061	1087668.05	3687788.71	1.528	1.780	0.252	1.696	0.168
6	a5060	1087670.65	3687792.35	1.523	1.780	0.257	1.696	0.173
7	a5059	1087671.42	3687797.59	1.521	1.780	0.259	1.696	0.175
8	a5058	1087671.84	3687803.58	1.576	1.780	0.204	1.696	0.120
9	a5057	1087672.92	3687806.36	1.579	1.780	0.201	1.696	0.117
10	a5056	1087674.57	3687810.67	1.561	1.780	0.219	1.696	0.135
11	VX557	1087676.41	3687815.00	1.563	1.780	0.217	1.696	0.133
12	VX556	1087676.87	3687817.39	1.503	1.780	0.277	1.696	0.193
13	VX555	1087676.75	3687820.00	1.501	1.780	0.279	1.696	0.195
14	VX554	1087677.14	3687822.44	1.530	1.780	0.250	1.696	0.166
					Average Difference	0.231	Average Difference	0.147
					Standard Deviation	0.035	Standard Deviation	0.035

Table 3A. Wrack line GPS point data for 2011 Hurricane Irene at Site E with NAD83 HARN Virginia State Plane South coordinates for northing and easting, sub-grid elevation, the base-grid maximum water level and the difference as inundation thickness, with and without 10% infiltration, including average and standard deviation statistics for verification of the sub-grid model with spatially-varying (SV) infiltration.

#	Wrack Line Point	Northing	Easting	Elevation (m)	Max Water Level without Infiltration (m)	Difference (m)	Max Water Level with SV Infiltration (m)	Difference with SV Infiltration (m)
1	VX566	1087565.305	3687330.905	1.520	1.785	0.265	1.721	0.201
2	VX565	1087568.984	3687335.120	1.592	1.785	0.193	1.721	0.129
3	VX564	1087570.099	3687340.301	1.626	1.785	0.159	1.721	0.095
4	VX563	1087569.918	3687347.885	1.630	1.785	0.155	1.721	0.091
5	VX562	1087569.774	3687354.096	1.653	1.785	0.132	1.721	0.068
6	VX561	1087569.723	3687363.956	1.635	1.785	0.150	1.721	0.086
7	a5063	1087570.539	3687390.786	1.665	1.785	0.120	1.721	0.056
					Average Difference	0.168	Average Difference	0.103
					Standard Deviation	0.049	Standard Deviation	0.049

Table 3B. Wrack line GPS point data for 2011 Hurricane Irene at Site F with NAD83 HARN Virginia State Plane South coordinates for northing and easting, sub-grid elevation, the base-grid maximum water level and the difference as inundation thickness, with and without 10% infiltration, including average and standard deviation statistics for verification of the sub-grid model with spatially-varying (SV) infiltration.

3.2 Conclusions

It is demonstrated that the hydrodynamic model UnTRIM with the sub-grid capability can be used as a hydrological transport model to channel the rainfall into a run-off transport model.

The UnTRIM2 model is capable of simulating storm surge and inundation at NASA Langley Research Center and at Langley Air Force Base utilizing the incorporation of Lidar data in a hydrodynamic and hydrological transport sub-grid model. Upon inclusion of precipitation data as an atmospheric model input, localized flooding in the interior of Langley was simulated (non-contiguous from storm surge flooding along the edge of the Back River estuary). Specific areas of localized precipitation-induced flooding persist in the southwest interior region of Langley Research Center. Although buildings have been filtered out of the Lidar topography data and the structure itself is not modeled, the resulting topography still includes localized raised elevations at the buildings. That means, precipitation will fall onto these raised elevations and water will navigate around the buildings and subsequently accumulate in the surrounding low-lying areas. Therefore, we believe that we have achieved adequate building-by-building flood predictions for NASA Facilities at NASA Langley Research Center.

Two simulated storm cases were compared utilizing past observation data. The 2003 Hurricane Isabel compared the impact of modeling storm surge with and without precipitation input as shown in Figure 2.3 A-C. Additionally, a series of simulations involving sea level rise associated with climate change specifically address Hurricane Isabel at +00in, +15in, +30in, and +60in as shown in Figures 2.6 A-D. The 2011 Hurricane Irene was compared with GPS wrack line observation data at six separate sites in a comprehensive inundation comparison between model prediction and observed locations of collected debris immediately after the storm as shown in Figures 2.9 A-F.

The Langley installed tidal gauges are valuable and important for benchmarking the water level surrounding NASA Langley and Air Force site both for tidal forcing and the storm induced variation. The comparison of model results and the Langley tide gauge was very satisfactory achieving a correlation coefficient of $R2 = 0.95$.

NASA-collected GPS wrack line observation data proves to be particularly useful for evaluating modeled inundation extent. It can be utilized in a rigorous comparison by calculating the difference between observed and model-predicted maximum inundation. When no infiltration is considered, the difference of the maximum water elevation is approximately 10%. The difference reduces to between 1 - 5% when 10% infiltration was considered; a reasonable runoff coefficient, considering the perennially high water table at NASA Langley Research Center.

3.3 Future Work

Future efforts will address the assumption of ignoring percolation of water through the soil, as currently all model surfaces are considered impermeable. Additionally, the assumption of no storm water drainage loss or underground pipes potentially neglects some potential for precipitation sinks not currently accounted for in the model grid. Also, buildings displayed in

Figures 2.9A-F have been filtered out of the Lidar topography data and are not present in the model sub-grid results. Provided accurate building heights, buildings potentially may be assessed in future model simulations for integration with the Lidar-derived sub-grid topography to determine their impact as barriers to maximum storm surge inundation.

Potential coupling with a large scale ocean model for future forecast simulation is essential to the improvement of model simulations. An operational forecast model using a large scale ocean model with interpolated forecast wind and pressure fields can provide predictive capability up to 30 hours in advance of a major storm. The large scale model can be utilized to provide necessary boundary conditions to run the localized high-resolution sub-grid model simulations for the Back River estuary. The utility of future forecast simulation for tropical and extra-tropical storm systems is valuable for emergency response and protection of valuable infrastructure. Finally, the model can also be used to answer important management questions:

- Do certain areas, tributaries, or small embayments tend to experience storm tide flooding to a greater degree or more frequently than others?
- Can risks be mitigated through improved planning or engineering?
- Are water-level extremes increased or locally prolonged because of increased runoff from modified watersheds?
- In conjunction with projected sea level rise, are particular regions of NASA Langley Research Center under greater threat of prolonged of more frequent inundation than others?

Acknowledgement:

The work was funded by NASA headquarters under the Climate Adaptation Science Investigator program administered by Jack Kaye. The Lidar data and wrack line measurement data was kindly provided by NASA Langley GIS team: Brad Ball and Berch Smithson.

Appendix A. Methodology and Model Setup

A1 Digital Elevation Model (DEM) derived from Lidar and Incorporation into Sub-Grid Model

The setup and design of the model domain for the Back River estuary is based upon Lidar topographic measurements from 2005 (Figure A.1, A – D). Lidar topography for NASA Langley came from 56 separate point cloud .las tiles in NAD83 HARN Virginia State Plane South in meters, with a vertical datum of NAVD88 in meters. The Lidar .las files were parsed as points and used to generate a single combined .xyz point file using las2txt from the Lastools toolset. The data sampled from the Lidar flyover for Langley are ample enough (at least one elevation value per m^2) for creation of a raster at 1m resolution bereft of frequent gaps in the data. The .xyz point file was utilized as an IDW power 2 interpolation input to a raster Geotiff file. Using the Lidar point cloud data, a raster was produced at 5m resolution. The resulting interpolation product was then translated from NAD83 HARN Virginia State Plane South coordinates to NAD83 CORS 96 in UTM Zone18N with a vertical datum of NAVD88 in meters for interpolation onto the model grid (Figure A.2).

The 5m Digital Elevation Model (DEM) produced from the Lidar data was cast over a domain covering the Back River system around NASA Langley with an open boundary at the mouth of the river leading into the Chesapeake Bay (Figure A.3). The base grid utilizes 50m resolution cells, with 100 nested 5x5m sub-grid cells within each base grid cell (Figure A.2). This base grid resolution was chosen so that the main stem of the Back River channel would have multiple grid cells across the width of the river for proper calculation of volume water transport into and out of the system. The sub-grid scaling was chosen such that the topographic Lidar-derived DEM would be at the native resolution (5m) and not require further interpolation and potentially invite computational error due to distortion. In the future, the Lidar point cloud can be utilized to produce even higher resolution DEMs down to 1m resolution. However, the error associated with Lidar data collection methods, assuming the most accurately calibrated instrumentation, still may include errors on the order of 0-10cm along spatially uniform terrain and 10-50cm in vegetated areas and urban environments.

Bathymetric .xyz point data (10m resolution) were retrieved from two NOAA bathymetric surveys of the Back River system, H07959 and H07185. Using ArcGIS 10.1, a power-2 inverse distance weighted interpolation was performed on the bathymetry data using a shoreline polyline as a barrier. The resulting interpolation product was then translated to NAD83 CORS 96 in UTM Zone18N with a vertical datum of NAVD88 in meters. With the Lidar-derived topography and NOAA bathymetry datasets in the same projections and datums, they are merged such that the bathymetric data would overlap the Lidar topographic data to resolve any issues with bridges or other impediments in the Lidar DEM potentially blocking proper water movement into rivers and streams second order and above. The resulting topography and bathymetry merged DEM was provided to grid-generation software, Janet v.2.9.36, to provide elevations for the model sub-grid, where the model domain was constructed with a 50m base grid with a 5m resolution sub-grid (Figure A.2).

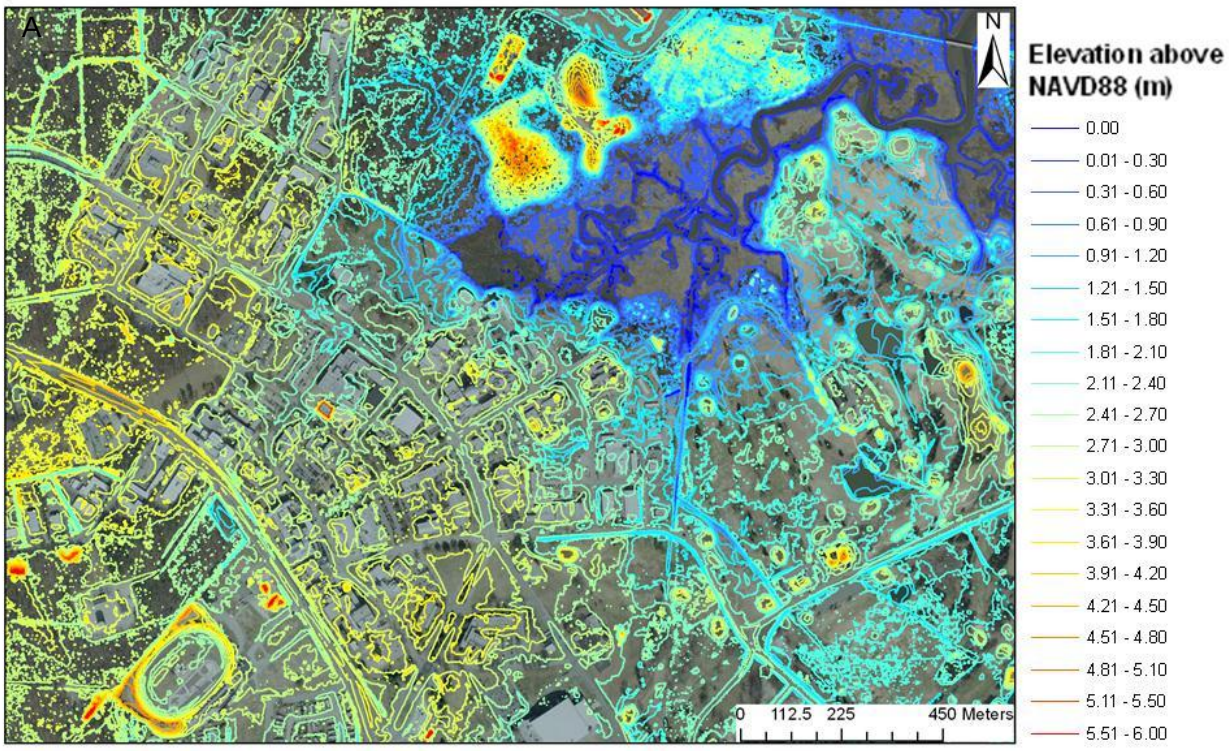

Figure A.1A. Lidar for Langley Research Center displaying 30cm vertical resolution contours.

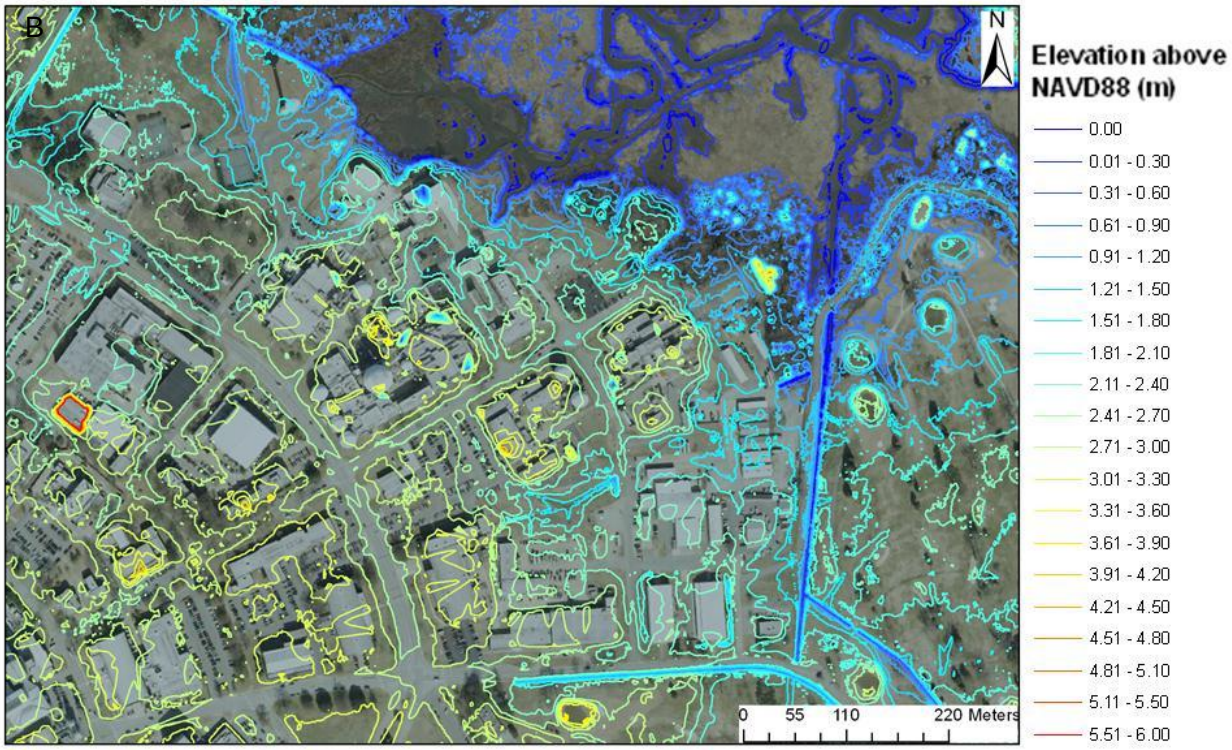

Figure A.1B. Lidar contours focused on central Langley Research Center displaying drainage ditches backing up to a meandering tidal creek along Back River.

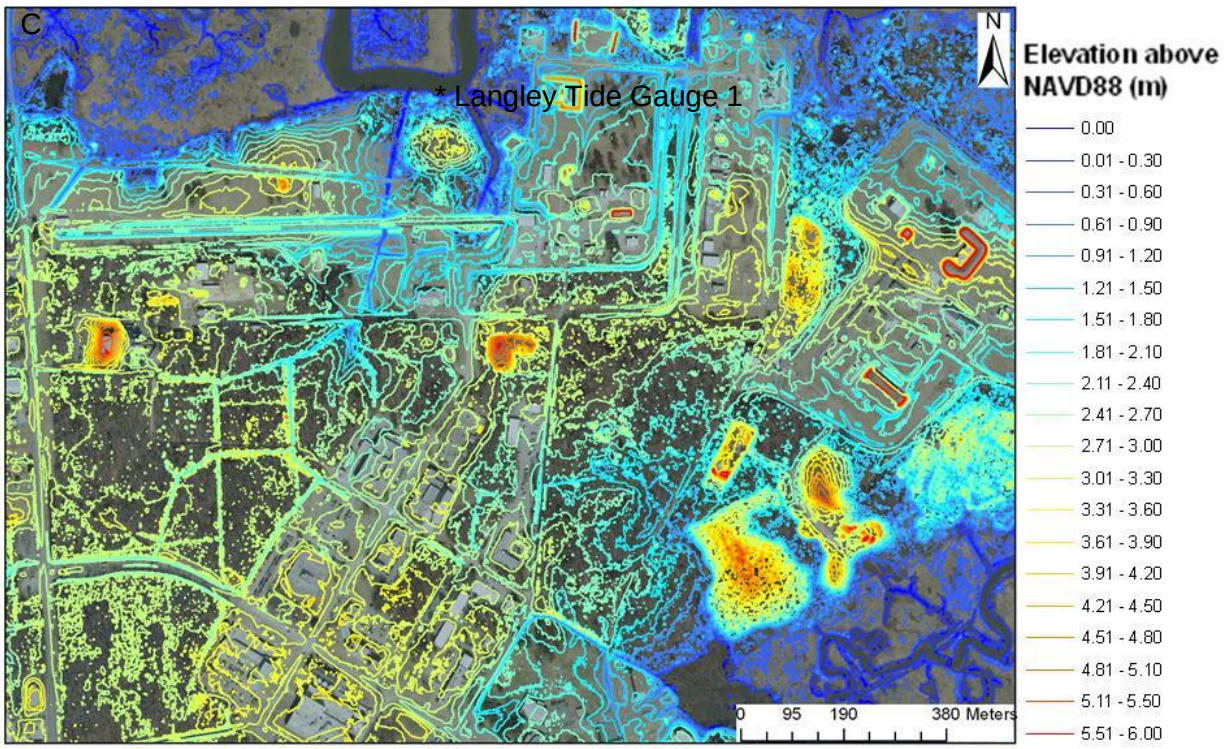

Figure A.1C. Lidar contours focused on the north end of Langley Research Center displaying drainage ditches near the location of the NASA Tide 01 tide gauge along Back River.

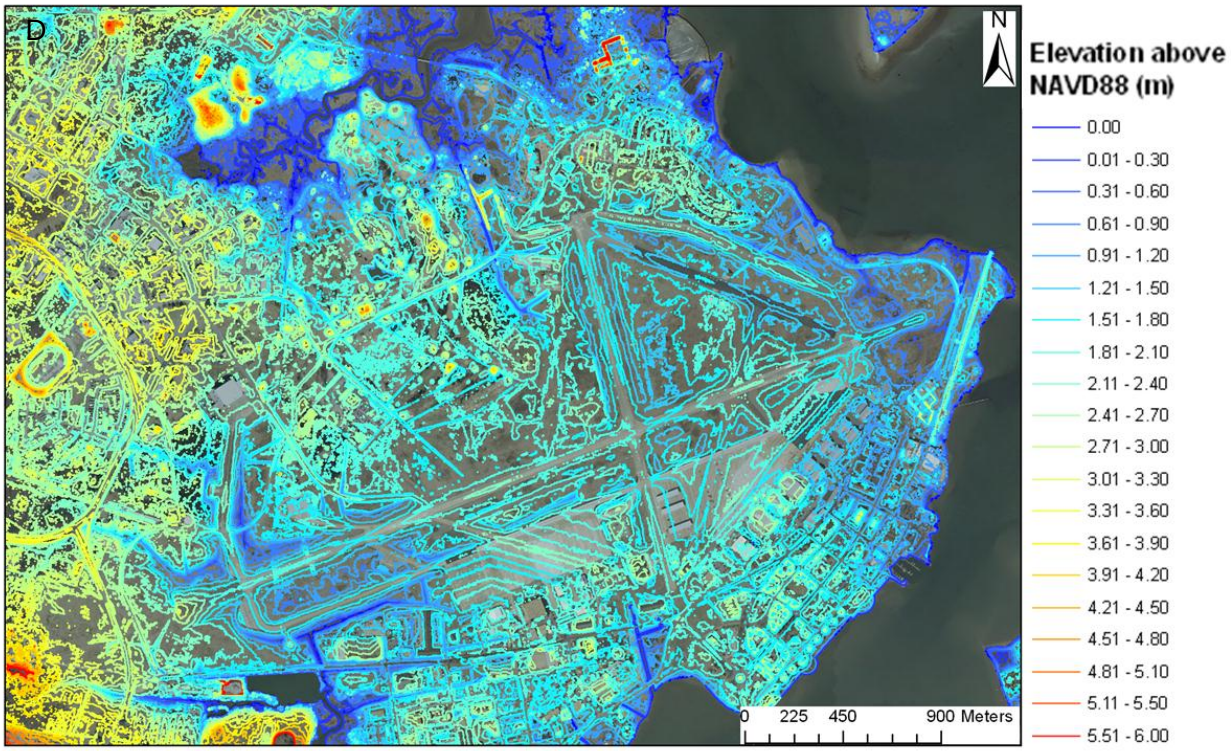

Figure A.1D. Peninsula contours shown for Langley Air Force Base and NASA Langley Research Center.

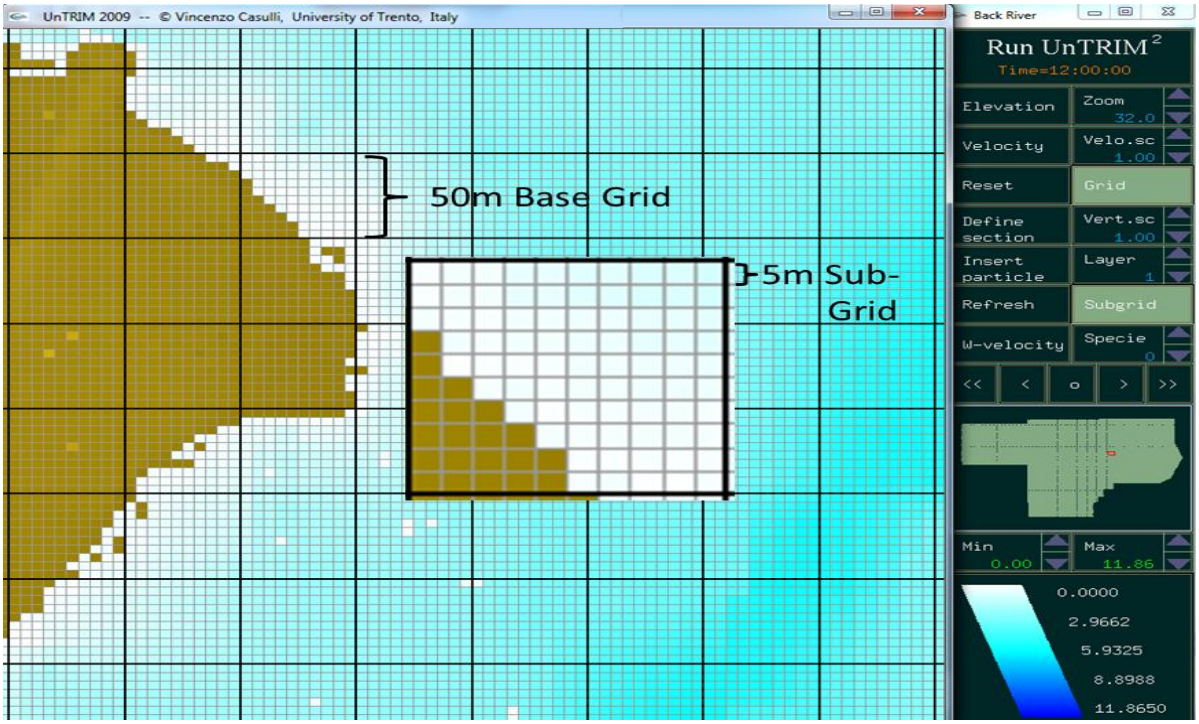

Figure A.2. 50m Base Grid shown with 5m Sub-Grid shown for the Northeast tip of Langley Air Force Base in the UnTRIM^2 model interface.

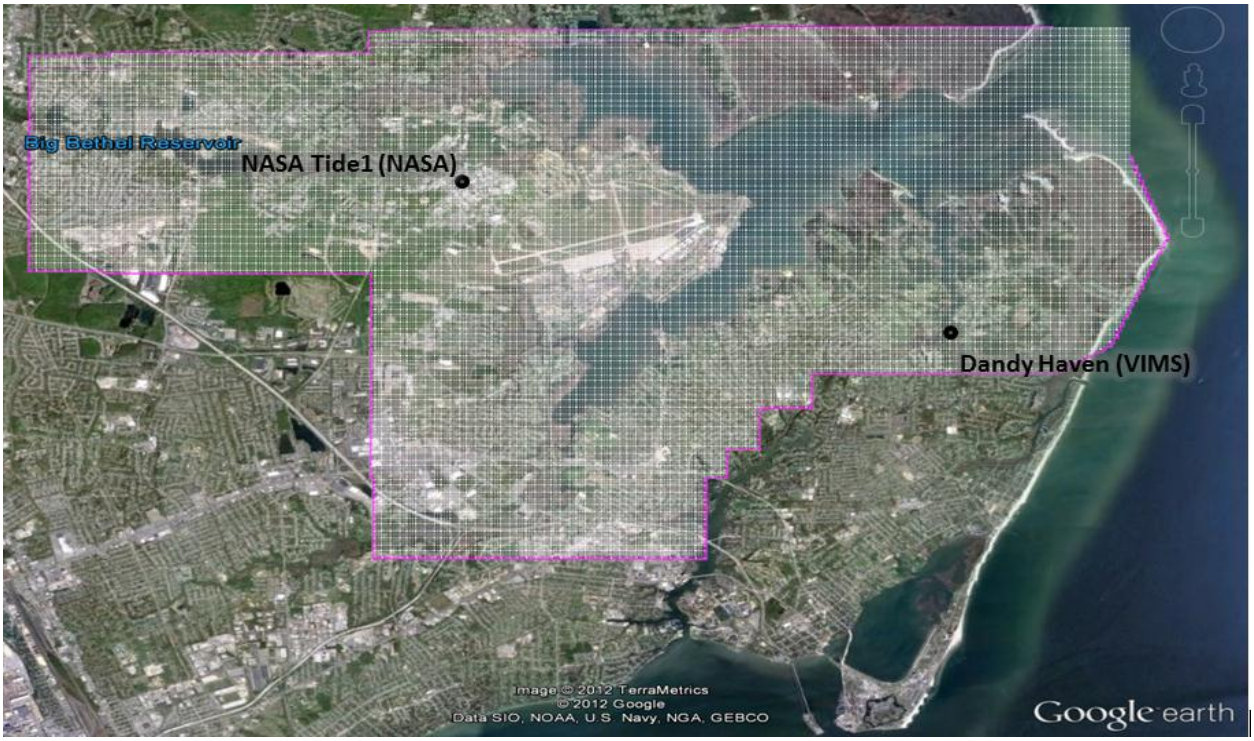

Figure A.3. Full Back River model domain in Google Earth with 54,057 nodes and 53,474 elements comprising the 50m resolution base grid, yielding 4,759,788 sub-grid elements at 5m resolution.

A2 Development of a Hydrological Transport Simulation with Precipitation

With the detail topography integrated into the hydrodynamic model sub-grid, as was done in the last section, the hydrodynamic model becomes a continuous time model that can be used to simulate the water budget given the landscapes in the watershed. UnTRIM^2 uses a two-level disaggregation scheme; a preliminary sub-basin identification is carried out based on topographic criteria, followed by further discretization using land use type considerations. When the precipitation is prescribed, it becomes a runoff model to describe the rainfall - runoff relations of a rainfall catchment area, watershed and drainage basin. More precisely, it produces the surface runoff hydrograph as a response to a rainfall hydrograph as input. In other words, the model calculates the conversion of rainfall into runoff. Often models have separate modules to address individual steps in the simulation process. The most common module is a subroutine for calculation of surface runoff, allowing variation in land use type, topography, soil type, vegetative cover, precipitation and land management practice (such as the application rate of a fertilizer). However, in this phase I approach, we will assume the land use is homogeneous and the soil is saturated during the storm condition.

Ideal test simulations for precipitation will be utilized to test the input of rainfall into the model in three separate cases: one using an open flow basin with rainfall shown in Figure A.4, one using a partially enclosed basin with rainfall in Figure A.5, and a closed flow basin with rainfall in Figure A.6. For all three simulations an ideal ditch has been designed with sloping sides angled into the basin as depicted in the inset of Figure A.6. The model grid is shaped like a sloping trough with a depth of 2m in the channel. The north and south banks of the trough gradually slope into the channel in the center with a maximum elevation of 2m on each side.

A2.1 Ideal Test Case with Open Flow Basin with Precipitation

The parameters for the open flow basin with rainfall ideal test case include a flux boundary condition with a constant prescribed 0.5 m/s flow on the west edge of the grid in Figure A.4 with no forcing at the open boundary on the east edge. A constant 25 mm/hr precipitation input was designated for a 72 hour simulation. Over the three day simulation, the UnTRIM2 model's particle tracking mode was utilized to place particles on the north and south banks of the ideal trough-shaped domain to allow precipitation to transport the particles into the channel to be transported out of the domain. The particles (red dots) are arbitrarily placed at a variety of elevations between 0-2m above the water level in the basin to ascertain if precipitation will gravitationally transport the particles perpendicular to the contours into the trough-shaped basin and out of the domain. This scenario was designed to demonstrate the model's capability of transporting precipitation into an unobstructed, free-flowing drainage ditch back to the neighboring river system.

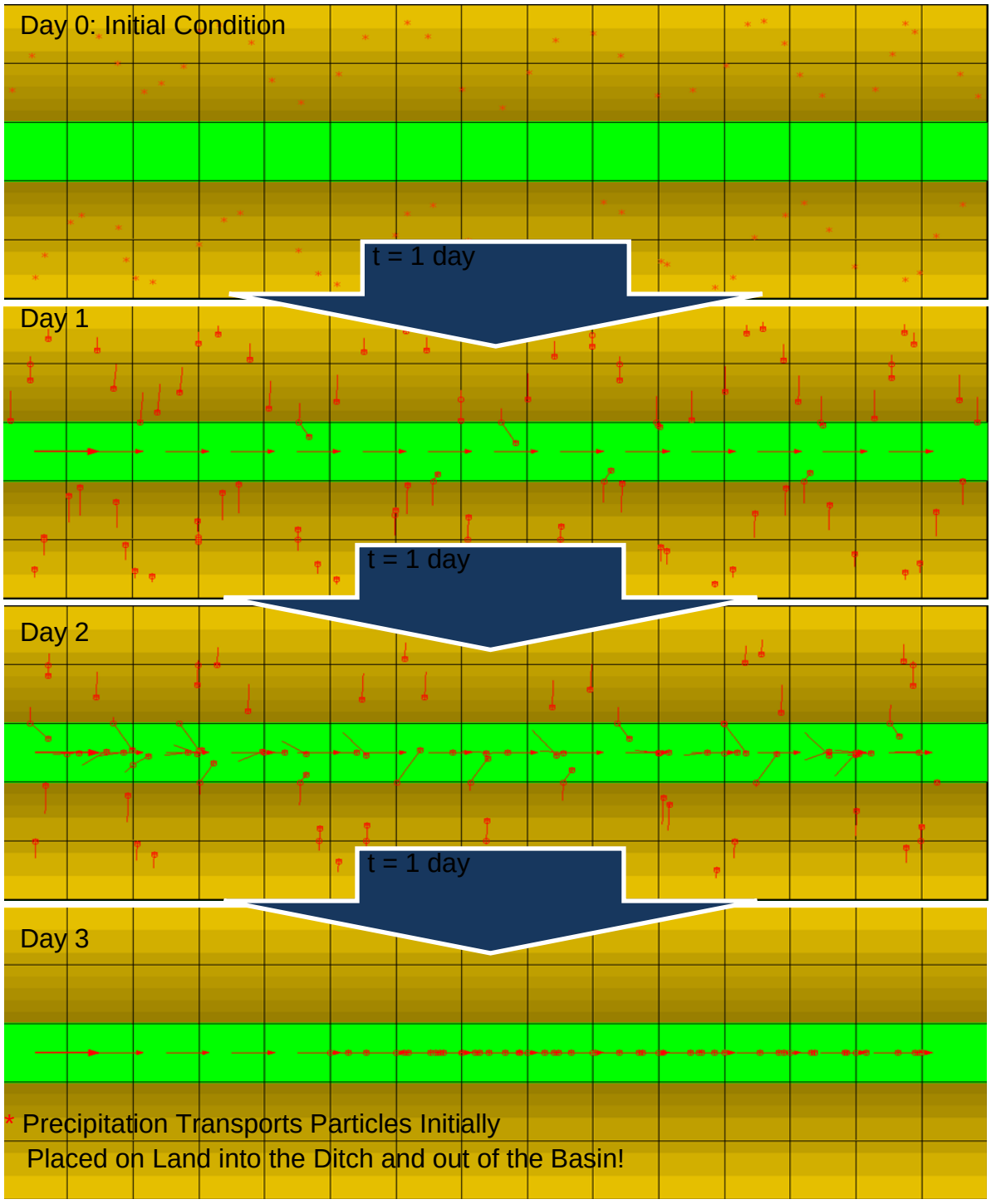

Figure A.4. Ideal test case for precipitation at 25 mm/hr in an open flow basin with a prescribed 0.5 m/s flow from the west.

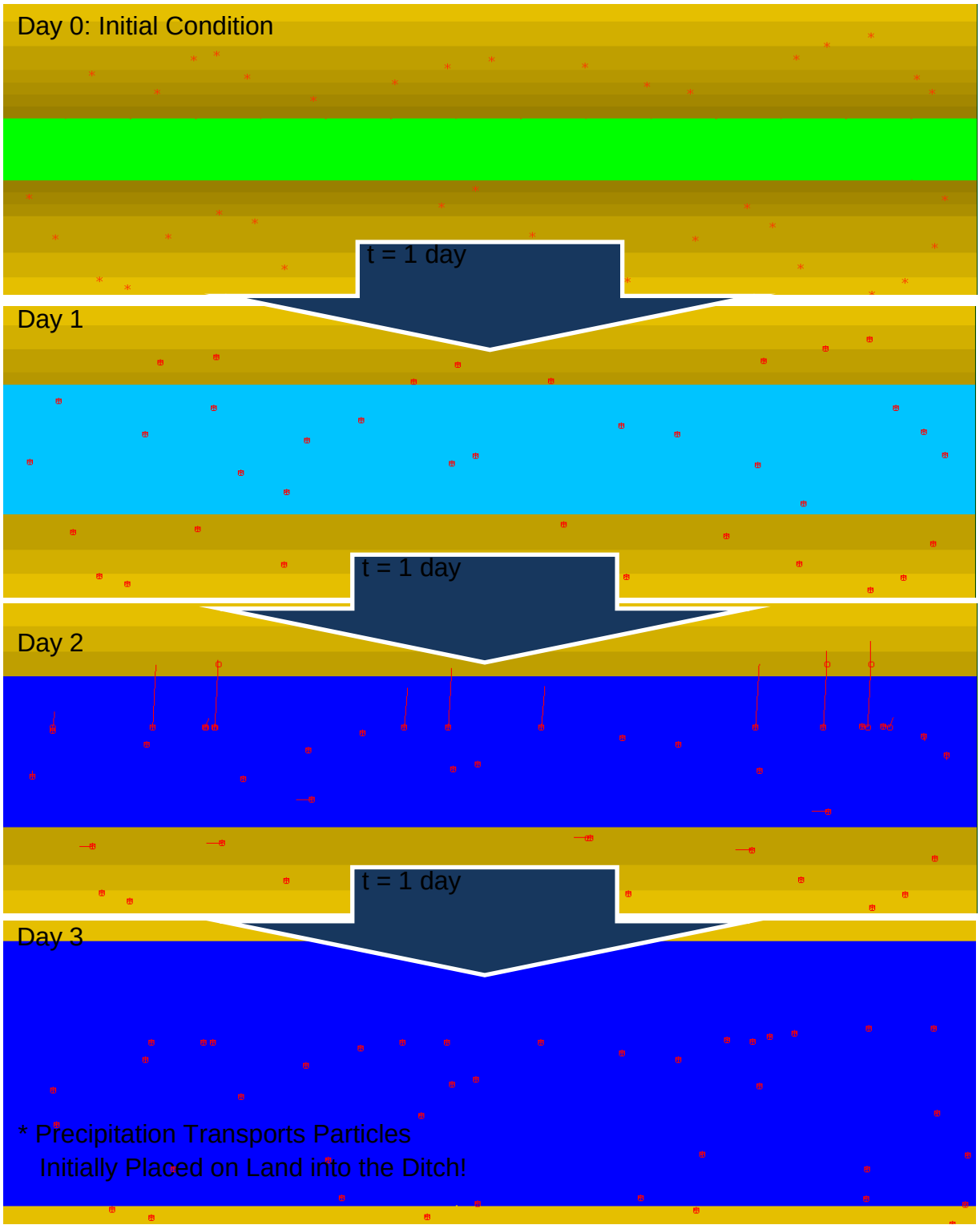

Figure A.5. Ideal test case for precipitation at 25 mm/hr in a partially enclosed basin with a wall along the west edge of the sloping trough basin.

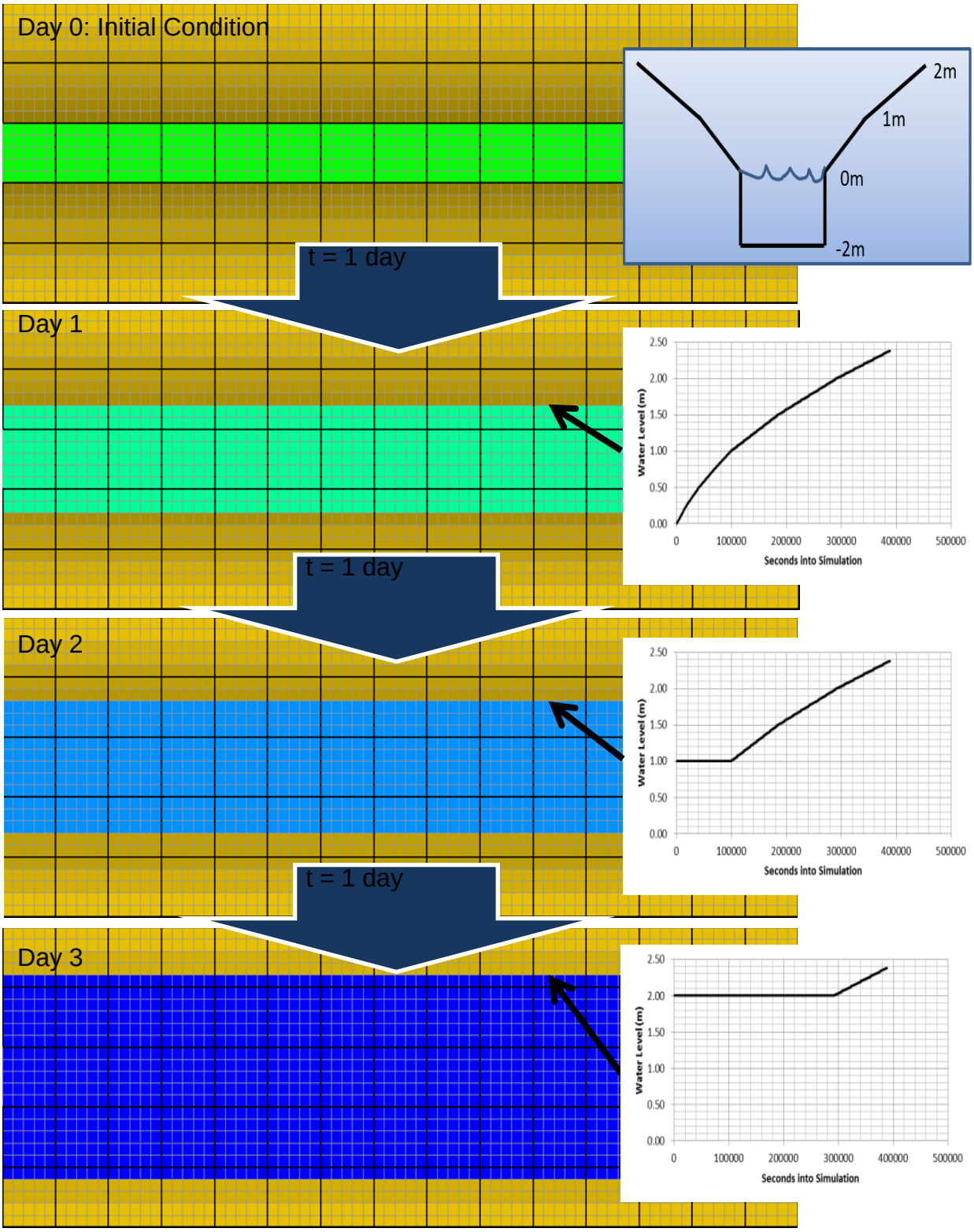

Figure A.6. Ideal test case for precipitation at 25 mm/hr in a fully enclosed basin which allows water volume to properly accumulate over time.

A2.2 Ideal Test Case for Partially Closed Basin with Precipitation

The parameters for the partially closed basin with precipitation as an ideal test case include a wall (or flux boundary condition with a prescribed 0 m/s flow) on the west edge of the grid shown in Figure A.5. As with the ideal test case for the open flow basin with rainfall, no forcing was prescribed at the open boundary on the eastern edge of the model domain with a constant 25 mm/hr precipitation rate designated for 72 hours in the simulation. The model's particle tracking mode was utilized again to arbitrarily place particles on the north and south banks of the trough-shaped domain between 0-2m above the water level in the basin to confirm that precipitation gravitationally transports the red particles into the trough-shaped basin and out of the domain. This scenario was designed to effectively demonstrate the model's capability of transporting precipitation into a partially obstructed drainage with an outlet ditch back to the neighboring river system. Unlike the previous simulation, the particles slowly collect in the channel, but only a small quantity of the particles exit the ditch, as virtually no current is observed in the ditch with one side (the west side) obstructed or otherwise blocked (Figure A.5).

A2.3 Ideal Test Case for Fully Enclosed Basin with Precipitation

In the case of an ideal test case with precipitation in a fully enclosed basin, there are walls blocking transport out of the domain on both sides of the idealized sloping trough with no prescribed flux boundary condition on the west edge of the grid, and no forcing at the clamped open boundary on the east edge. The same constant 25 mm/hr precipitation input was prescribed over the 72 hour simulation shown in Figure A.6. This test case was designed to test the conservation of mass and ascertain that precipitation would accumulate in a ditch if there is no outlet to allow water to escape. This scenario successfully validates the model's ability of collecting precipitation over time and allows the user to compute the volume of water collected over time in a simplistic bathtub-style simulation.

A3 Storm Tide and Inundation Model Forcing Functions

A3.1 Tidal Forcing

Tides are forced along the Back River open boundary on the easternmost edge of the domain at the mouth of Back River into the Chesapeake Bay with the north bank along the southeastern edge of Poquoson, and the south bank along the Grandview Park spit in Hampton shown in Figure A.3. Model application simulations for the 2003 Hurricane Isabel make use of NOAA observation data from Sewells Point, VA (Station #8638610), as the tidal boundary condition. This station was utilized as a tidal input at the open boundary of the Back River domain due to its harmonic similarity in tidal frequency relative to the mouth of the Chesapeake Bay and for its use in the calibration of the three recently installed Langley tide gauges (NASA Langley GIS Team, 2010, 2012). The tide input storm scenarios were the 2009 November Nor'easter (Nor'Ida), and 2011 Hurricane Irene and were collected 3km from the model's open boundary shown in Figure A.3. This tide gauge is located in the Back River estuary at Dandy Haven Marina (courtesy of VIMS TideWatch), and interpolated to a 5 minute time step (Table A1, Appendix A).

A3.2 Atmospheric Wind, Pressure, and Precipitation Forcing

Wind data were retrieved in m/s from NOAA observations at Sewell's Point, VA (Station #8638610) and prepared as a uniform input throughout the domain for each of the storm scenarios. U and V wind velocities were extracted and wind fields were interpolated to 5 minute intervals for each of the storm scenarios with appropriate start and end times for each storm event included in Table A1. Atmospheric pressure data in mbars were obtained for the same time periods from NOAA observations at Sewell's Point, VA as well. Pressure data were converted to Pascals, and prescribed as a uniform atmospheric pressure input throughout the domain. Precipitation inputs were interpolated from hourly measurements from the NOAA NGDC collection station at the Williamsburg/Newport News Airport nearby NASA Langley.

A.4 Verification of Results

Tide stations Langley Tide1 and Back River Dandy Haven (part of a suite of VIMS TideWatch stations throughout the Chesapeake Bay) will be utilized to evaluate the temporal variability of each storm system in Table A1. The Langley Tide gauge 1 was installed in 2010, and the Back River Dandy Haven Gauge was installed in 2008 with their locations noted within the model domain in Figure A.3 (NASA Langley GIS Team, 2010). It should be noted that Langley has recently installed 2 additional tide gauges (NASA Tide2 and NASA Tide3) within the model domain in April 2012, but they are not included due to their recent installation and non-presence during any the storm events noted in Table A1 (NASA Langley GIS Team, 2012). An R^2 correlation will be utilized to compare the observations with the model result for each scenario as a statistical measure of accuracy. Statistical tests for spatial verification of model coastal flooding results will utilize GPS wrack line data (collected via GPS using debris presence after each storm) to assess the maximum extent of inundation.

Table A1. Chart of various storm scenarios conducted in the vicinity of NASA Langley Research Center with model start and end times in Greenwich Mean Time (GMT).

	Storm Scenario	Simulation Date Range	
		Start Time	End Time
1	2003 Hurricane Isabel	00:00 GMT 09/01/2009	00:00 GMT 10/01/2009
2	2009 November Nor'easter	00:00 GMT 11/01/2009	00:00 GMT 12/01/2009
3	2011 Hurricane Irene	00:00 GMT 08/01/2011	00:00 GMT 09/01/2011

Appendix B: COMPARISON BETWEEN WRACK LINE MEASUREMENT AND PREDICTED MAXIMUM WATER LEVEL

#	Wrack Line Point	Northing	Easting	Elevation (m)	Max Water Level without Infiltration (m)	Difference (m)	Max Water Level with 10% Infiltration (m)	Difference with 10% Infiltration (m)
1	a5027	1086519.375	3688608.584	1.627	1.802	0.175	1.622	-0.005
2	a5028	1086517.371	3688609.014	1.679	1.802	0.123	1.622	-0.057
3	VX519	1086516.091	3688610.823	1.702	1.802	0.1	1.622	-0.080
4	VX518	1086516.126	3688611.563	1.683	1.802	0.119	1.622	-0.061
5	VX517	1086516.076	3688612.504	1.665	1.802	0.137	1.622	-0.043
6	VX516	1086515.458	3688613.648	1.695	1.802	0.107	1.622	-0.073
7	VX515	1086514.373	3688614.778	1.686	1.802	0.116	1.622	-0.064
8	VX514	1086513.578	3688616.071	1.706	1.802	0.096	1.622	-0.084
9	a5026	1086513.997	3688622.987	1.724	1.802	0.078	1.622	-0.102
10	a5025	1086516.533	3688628.9	1.739	1.802	0.063	1.622	-0.117
11	a5024	1086515.484	3688635.438	1.705	1.802	0.097	1.622	-0.083
12	a5023	1086515.647	3688637.976	1.723	1.802	0.079	1.622	-0.101
13	a5022	1086512.812	3688641.324	1.667	1.802	0.135	1.622	-0.045
14	a5021	1086508.635	3688643.482	1.717	1.802	0.085	1.622	-0.095
15	a5020	1086507.836	3688648.444	1.7	1.802	0.102	1.622	-0.078
16	a5019	1086507.545	3688655.408	1.694	1.802	0.108	1.622	-0.072
17	a5018	1086508.05	3688659.18	1.681	1.802	0.121	1.622	-0.059
18	a5017	1086508.953	3688663.616	1.699	1.802	0.103	1.622	-0.077
19	a5016	1086510.462	3688667.204	1.695	1.802	0.107	1.622	-0.073
20	a5015	1086510.789	3688670.572	1.694	1.802	0.108	1.622	-0.072
21	a5014	1086511.676	3688674.6	1.646	1.802	0.156	1.622	-0.024
22	VX513	1086515.103	3688683.796	1.634	1.802	0.168	1.622	-0.012
23	VX512	1086514.783	3688684.566	1.635	1.802	0.167	1.622	-0.013
24	VX511	1086514.213	3688685.837	1.647	1.802	0.155	1.622	-0.025
25	VX510	1086513.448	3688687.233	1.654	1.802	0.148	1.622	-0.032
26	VX509	1086513.072	3688688.397	1.666	1.802	0.136	1.622	-0.044
27	VX508	1086510.753	3688690.108	1.647	1.802	0.155	1.622	-0.025
28	VX507	1086510.896	3688691.597	1.672	1.802	0.13	1.622	-0.050

29	VX506	1086510.73	3688692.998	1.657	1.802	0.145	1.622	-0.035
30	VX505	1086510.577	3688694.43	1.632	1.802	0.17	1.622	-0.010
31	VX504	1086510.9	3688696.027	1.615	1.802	0.187	1.622	0.007
32	VX503	1086510.715	3688697.605	1.671	1.802	0.131	1.622	-0.049
33	VX502	1086510.801	3688699.177	1.649	1.802	0.153	1.622	-0.027
34	VX501	1086510.729	3688700.721	1.643	1.802	0.159	1.622	-0.021
35	VX500	1086510.434	3688701.786	1.635	1.802	0.167	1.622	-0.013
					Average	0.128	Average	-0.052
					Standard	0.032	Standard	0.032

Table B1. Wrack line GPS point data at Site A with NAD83 HARN Virginia State Plane South coordinates for northing and easting, sub-grid elevation, the base-grid maximum water level and the difference as inundation thickness, with and without 10% infiltration, including average and standard deviation statistics for verification of the sub-grid model.

#	Wrack Line Point	Northing	Easting	Elevation (m)	Max Water Level without Infiltration (m)	Difference (m)	Max Water Level with 10% Infiltration (m)	Difference with 10% Infiltration (m)
1	VX532	1086594.643	3688370.591	1.750	1.801	0.051	1.621	-0.129
2	VX531	1086597.287	3688374.649	1.746	1.801	0.055	1.621	-0.125
3	VX530	1086598.288	3688378.817	1.750	1.801	0.051	1.621	-0.129
4	VX529	1086599.157	3688383.034	1.749	1.801	0.052	1.621	-0.128
5	VX528	1086600.463	3688388.673	1.759	1.801	0.042	1.621	-0.138
6	a5036	1086575.220	3688398.068	1.669	1.801	0.132	1.621	-0.048
7	a5040	1086595.261	3688399.296	1.751	1.801	0.050	1.621	-0.130
8	a5039	1086593.454	3688400.210	1.750	1.801	0.051	1.621	-0.129
9	a5038	1086590.768	3688400.983	1.755	1.801	0.046	1.621	-0.134
10	a5037	1086588.065	3688401.060	1.764	1.801	0.037	1.621	-0.143
11	a5035	1086578.106	3688405.365	1.663	1.801	0.138	1.621	-0.042
12	a5034	1086577.494	3688409.574	1.661	1.801	0.140	1.621	-0.040
13	a5033	1086578.844	3688414.090	1.674	1.801	0.127	1.621	-0.053
14	a5032	1086578.522	3688418.064	1.671	1.801	0.130	1.621	-0.050
15	a5029	1086560.682	3688421.860	1.654	1.801	0.147	1.621	-0.033
16	a5030	1086564.393	3688422.012	1.668	1.801	0.133	1.621	-0.047

17	a5031	1086571.994	3688422.993	1.686	1.801	0.115	1.621	-0.065
18	VX520	1086536.219	3688423.552	1.645	1.801	0.156	1.621	-0.024
19	VX521	1086540.460	3688426.264	1.669	1.801	0.132	1.621	-0.048
20	VX522	1086544.949	3688429.776	1.639	1.801	0.162	1.621	-0.018
21	VX523	1086551.865	3688434.625	1.670	1.801	0.131	1.621	-0.049
22	VX524	1086557.694	3688438.474	1.631	1.801	0.170	1.621	-0.010
23	VX525	1086560.314	3688441.591	1.654	1.801	0.147	1.621	-0.033
24	VX526	1086562.895	3688442.864	1.631	1.801	0.170	1.621	-0.010
25	VX527	1086565.371	3688443.812	1.604	1.801	0.197	1.621	0.017
					Average	0.110	Average	-0.070
					Standard	0.050	Standard	0.050

Table B2. Wrack line GPS point data at Site B with NAD83 HARN Virginia State Plane South coordinates for northing and easting, sub-grid elevation, the base-grid maximum water level and the difference as inundation thickness, with and without 10% infiltration, including average and standard deviation statistics for verification of the sub-grid model.

#	Wrack Line Point	Northing	Easting	Elevation (m)	Max Water Level without Infiltration (m)	Difference (m)	Max Water Level with 10% Infiltration (m)	Difference with 10% Infiltration (m)
1	VX553	1087857.664	3688508.326	1.590	1.766	0.176	1.589	-0.001
2	VX552	1087854.880	3688515.822	1.594	1.766	0.172	1.589	-0.005
3	VX551	1087853.441	3688521.385	1.574	1.766	0.192	1.589	0.015
4	VX550	1087852.618	3688525.460	1.543	1.766	0.223	1.589	0.046
5	VX549	1087853.282	3688532.202	1.580	1.766	0.186	1.589	0.009
6	VX548	1087855.684	3688536.171	1.616	1.766	0.150	1.589	-0.027
7	VX547	1087856.630	3688540.129	1.640	1.766	0.126	1.589	-0.051
8	VX546	1087855.921	3688544.541	1.639	1.766	0.127	1.589	-0.050
9	VX545	1087854.189	3688550.450	1.632	1.766	0.134	1.589	-0.043
10	VX544	1087850.881	3688556.263	1.640	1.766	0.126	1.589	-0.051
11	VX543	1087849.485	3688562.785	1.588	1.766	0.178	1.589	0.001

12	VX542	1087845.848	3688566.306	1.584	1.766	0.182	1.589	0.005
13	VX541	1087847.462	3688571.618	1.637	1.766	0.129	1.589	-0.048
14	VX540	1087845.286	3688573.756	1.634	1.766	0.132	1.589	-0.045
15	VX539	1087844.478	3688577.683	1.566	1.766	0.200	1.589	0.023
16	VX537	1087828.872	3688580.495	1.544	1.766	0.222	1.589	0.045
17	VX538	1087832.782	3688580.816	1.509	1.766	0.257	1.589	0.080
18	VX536	1087818.186	3688582.003	1.574	1.766	0.192	1.589	0.015
19	VX535	1087812.782	3688584.123	1.572	1.766	0.194	1.589	0.017
20	VX534	1087807.102	3688586.422	1.599	1.766	0.167	1.589	-0.010
21	VX533	1087801.790	3688588.476	1.575	1.766	0.191	1.589	0.014
22	a5051	1087815.832	3688607.961	1.473	1.766	0.293	1.589	0.116
23	a5050	1087817.645	3688609.878	1.531	1.766	0.235	1.589	0.058
24	a5049	1087819.673	3688615.755	1.720	1.766	0.046	1.589	-0.131
25	a5048	1087816.891	3688616.656	1.691	1.766	0.075	1.589	-0.102
26	a5047	1087813.098	3688617.414	1.634	1.766	0.132	1.589	-0.045
27	a5046	1087809.551	3688619.224	1.623	1.766	0.143	1.589	-0.034
28	a5045	1087808.063	3688620.189	1.625	1.766	0.141	1.589	-0.036
29	a5044	1087807.875	3688622.824	1.619	1.766	0.147	1.589	-0.030
30	a5043	1087806.676	3688624.209	1.625	1.766	0.141	1.589	-0.036
31	a5042	1087804.188	3688626.321	1.618	1.766	0.148	1.589	-0.029
32	a5041	1087800.942	3688627.558	1.595	1.766	0.171	1.589	-0.006
					Average Difference	0.167	Average Difference	-0.010
					Standard Deviation	0.049	Standard Deviation	0.049

Table B3. Wrack line GPS point data at Site C with NAD83 HARN Virginia State Plane South coordinates for northing and easting, sub-grid elevation, the base-grid maximum water level and the difference as inundation thickness, with and without 10% infiltration, including average and standard deviation statistics for verification of the sub-grid model.

#	Wrack Line Point	Northing	Easting	Elevation (m)	Max Water Level without Infiltration (m)	Difference (m)	Max Water Level with 10% Infiltration (m)	Difference with 10% Infiltration (m)
1	a5055	1087804.297	3688174.532	1.569	1.775	0.21	1.598	0.029
2	a5054	1087802.715	3688179.124	1.572	1.775	0.20	1.598	0.025
3	a5053	1087801.440	3688184.098	1.571	1.775	0.20	1.598	0.027
4	a5052	1087802.098	3688187.626	1.482	1.775	0.29	1.598	0.116
					Average Difference	0.227	Average Difference	0.049
					Standard Deviation	0.044	Standard Deviation	0.044

Table B4. Wrack line GPS point data at Site D with NAD83 HARN Virginia State Plane South coordinates for northing and easting, sub-grid elevation, the base-grid maximum water level and the difference as inundation thickness, with and without 10% infiltration, including average and standard deviation statistics for verification of the sub-grid model.

#	Wrack Line Point	Northing	Easting	Elevation (m)	Max Water Level without Infiltration (m)	Difference (m)	Max Water Level with 10% Infiltration (m)	Difference with 10% Infiltration (m)
1	VX558	1087664.557	3687772.846	1.531	1.780	0.249	1.602	0.071
2	VX559	1087663.204	3687778.586	1.594	1.780	0.186	1.602	0.008
3	VX560	1087663.255	3687781.840	1.618	1.780	0.162	1.602	-0.016
4	a5062	1087666.592	3687787.504	1.554	1.780	0.226	1.602	0.048
5	a5061	1087668.057	3687788.712	1.528	1.780	0.252	1.602	0.074
6	a5060	1087670.659	3687792.356	1.523	1.780	0.257	1.602	0.079
7	a5059	1087671.423	3687797.591	1.521	1.780	0.259	1.602	0.081
8	a5058	1087671.842	3687803.581	1.576	1.780	0.204	1.602	0.026
9	a5057	1087672.926	3687806.364	1.579	1.780	0.201	1.602	0.023
10	a5056	1087674.576	3687810.679	1.561	1.780	0.219	1.602	0.041

11	VX557	1087676.411	3687815.002	1.563	1.780	0.217	1.602	0.039
12	VX556	1087676.875	3687817.396	1.503	1.780	0.277	1.602	0.099
13	VX555	1087676.758	3687820.006	1.501	1.780	0.279	1.602	0.101
14	VX554	1087677.144	3687822.442	1.530	1.780	0.250	1.602	0.072
					Average Difference	0.231	Average Difference	0.053
					Standard	0.035	Standard	0.035

Table B5. Wrack line GPS point data at Site E with NAD83 HARN Virginia State Plane South coordinates for northing and easting, sub-grid elevation, the base-grid maximum water level and the difference as inundation thickness, with and without 10% infiltration, including average and standard deviation statistics for verification of the sub-grid model.

#	Wrack Line Point	Northing	Easting	Elevation (m)	Max Water Level without Infiltration (m)	Difference (m)	Max Water Level with 10% Infiltration (m)	Difference with 10% Infiltration (m)
1	VX566	1087565.305	3687330.905	1.520	1.785	0.265	1.607	0.087
2	VX565	1087568.984	3687335.120	1.592	1.785	0.193	1.607	0.015
3	VX564	1087570.099	3687340.301	1.626	1.785	0.159	1.607	-0.019
4	VX563	1087569.918	3687347.885	1.630	1.785	0.155	1.607	-0.023
5	VX562	1087569.774	3687354.096	1.653	1.785	0.132	1.607	-0.047
6	VX561	1087569.723	3687363.956	1.635	1.785	0.150	1.607	-0.029
7	a5063	1087570.539	3687390.786	1.665	1.785	0.120	1.607	-0.059
					Average Difference	0.168	Average Difference	-0.011
					Standard Deviation	0.049	Standard Deviation	0.049

Table B6. Wrack line GPS point data at Site F with NAD83 HARN Virginia State Plane South coordinates for northing and easting, sub-grid elevation, the base-grid maximum water level and the difference as inundation thickness, with and without 10% infiltration, including average and standard deviation statistics for verification of the sub-grid model.

References:

Casulli, V. and Sterling, G. S. (2011): “Semi-implicit sub-grid modeling of three-dimensional free-surface flows”, *International journal for numerical method in fluids*. Vol. 67, p441-449.

CIPS report by Sellner, Kevin, Elizabeth Smith, Harry V. Wang, Ming Li, Jay Titlow, and Barry Stamey (2012): “Chesapeake Inundation Prediction System (CIPS): flood forecasts for coastal-bay-estuary resiliency to storm surge”. Final report submitted to *NOAA IOOS Program* Office; award number: NOAA NA07NOS4730214.

Cho Kyoung-Ho, Harry Wang Jian Shen, Arnoldo Valle-Levinson and Yi-cheng Teng (2012): “A modeling study on the response of the Chesapeake Bay to Hurricane Events of Floyd and Isabel” *Ocean Modeling, Vol. 49-50, p22-46.*

National Land Cover Database, 2006. NOAA Coastal Change Analysis Program. www.csc.noaa.gov/landcover .

NASA Langley GIS Team, 2010. LaRC Prototype Tide Measurement Station. Langley Research Center, Hampton, VA 23681-0001, M/S 300. http://capable.larc.nasa.gov/tide-gauge/docs-pdf/Langley_sea_level_gauge_report.pdf .

NASA Langley GIS Team, 2012. LaRC Tide Measurement Stations. Langley Research Center, Hampton, VA 23681-0001, M/S 300. http://capable.larc.nasa.gov/tide-gauge/docs-pdf/New_stations_report.pdf .

Roland, Aron, Yinglong. Zhang, Harry. V. Wang, Yanqiu Meng, Yi-cheng Teng, Vladimir Maderichd, Igor Brovchenkod, Mathieu Dutour-Sikirice and Ulrich Zankea (2012): “A fully coupled 3D wave-current interaction model on unstructured grids". JGR – Oceans, Vol. 117, C00J33, doi:10.1029/2012

REPORT DOCUMENTATION PAGE

Form Approved
OMB No. 0704-0188

1. REPORT DATE *(DD-MM-YYYY)*	2. REPORT TYPE	3. DATES COVERED *(From - To)*
01- 10 - 2013	Technical Memorandum	

4. TITLE AND SUBTITLE

A Storm Surge and Inundation Model of the Back River Watershed at NASA Langley Research Center

5a. CONTRACT NUMBER

5b. GRANT NUMBER

5c. PROGRAM ELEMENT NUMBER

6. AUTHOR(S)

Loftis, Jon Derek; Wang, Harry V.; DeYoung, Russell J.

5d. PROJECT NUMBER

5e. TASK NUMBER

5f. WORK UNIT NUMBER

509496.02.08.03.69

7. PERFORMING ORGANIZATION NAME(S) AND ADDRESS(ES)

NASA Langley Research Center
Hampton, VA 23681-2199

8. PERFORMING ORGANIZATION REPORT NUMBER

L-20243

9. SPONSORING/MONITORING AGENCY NAME(S) AND ADDRESS(ES)

National Aeronautics and Space Administration
Washington, DC 20546-0001

10. SPONSOR/MONITOR'S ACRONYM(S)

NASA

11. SPONSOR/MONITOR'S REPORT NUMBER(S)

NASA/TM-2013-218046

12. DISTRIBUTION/AVAILABILITY STATEMENT

Unclassified - Unlimited
Subject Category 47
Availability: NASA CASI (443) 757-5802

13. SUPPLEMENTARY NOTES

14. ABSTRACT

This report on a Virginia Institute for Marine Science project demonstrates that the sub-grid modeling technology (now as part of Chesapeake Bay Inundation Prediction System, CIPS) can incorporate high-resolution Lidar measurements provided by NASA Langley Research Center into the sub-grid model framework to resolve detailed topographic features for use as a hydrological transport model for run-off simulations within NASA Langley and Langley Air Force Base. The rainfall over land accumulates in the ditches/channels resolved via the model sub-grid was tested to simulate the run-off induced by heavy precipitation. Possessing both the capabilities for storm surge and run-off simulations, the CIPS model was then applied to simulate real storm events starting with Hurricane Isabel in 2003. It will be shown that the model can generate highly accurate on-land inundation maps as demonstrated by excellent comparison of the Langley tidal gauge time series data (CAPABLE.larc.nasa.gov) and spatial patterns of real storm wrack line measurements with the model results simulated during Hurricanes Isabel (2003), Irene (2011), and a 2009 Nor'easter. With confidence built upon the model's performance, sea level rise scenarios from the ICCP (International Climate Change Partnership) were also included in the model scenario runs to simulate future inundation cases.

15. SUBJECT TERMS

Climate change; Flood model; Hurricanes; Storm surge; Storms

16. SECURITY CLASSIFICATION OF:			17. LIMITATION OF ABSTRACT	18. NUMBER OF PAGES	19a. NAME OF RESPONSIBLE PERSON
a. REPORT	b. ABSTRACT	c. THIS PAGE			STI Help Desk (email: help@sti.nasa.gov)
					19b. TELEPHONE NUMBER *(Include area code)*
U	U	U	UU	62	(443) 757-5802